
Fraunhofer Institut
Techno- und
Wirtschaftsmathematik

A. Scherrer, K.-H. Küfer, M. Monz, F. Alonso,
T. Bortfeld

# IMRT planning on adaptive volume structures – a significant advance of computational complexity

Berichte des Fraunhofer ITWM, Nr. 60 (2004)

ISSN 1434-9973

Bericht 60 (2004)



Die Veröffentlichungen in der Berichtsreihe des Fraunhofer ITWM können bezogen werden über:

Fraunhofer-Institut für Techno- und
Wirtschaftsmathematik ITWM
Gottlieb-Daimler-Straße, Geb. 49

67663 Kaiserslautern
Germany

Telefon: +49 (0) 6 31/2 05-32 42
Telefax: +49 (0) 6 31/2 05-41 39
E-Mail: info@itwm.fraunhofer.de
Internet: www.itwm.fraunhofer.de

# Vorwort

Das Tätigkeitsfeld des Fraunhofer Instituts für Techno- und Wirtschaftsmathematik ITWM umfasst anwendungsnahe Grundlagenforschung, angewandte Forschung sowie Beratung und kundenspezifische Lösungen auf allen Gebieten, die für Techno- und Wirtschaftsmathematik bedeutsam sind.

In der Reihe »Berichte des Fraunhofer ITWM« soll die Arbeit des Instituts kontinuierlich einer interessierten Öffentlichkeit in Industrie, Wirtschaft und Wissenschaft vorgestellt werden. Durch die enge Verzahnung mit dem Fachbereich Mathematik der Universität Kaiserslautern sowie durch zahlreiche Kooperationen mit internationalen Institutionen und Hochschulen in den Bereichen Ausbildung und Forschung ist ein großes Potenzial für Forschungsberichte vorhanden. In die Berichtreihe sollen sowohl hervorragende Diplom- und Projektarbeiten und Dissertationen als auch Forschungsberichte der Institutsmitarbeiter und Institutsgäste zu aktuellen Fragen der Techno- und Wirtschaftsmathematik aufgenommen werden.

Darüberhinaus bietet die Reihe ein Forum für die Berichterstattung über die zahlreichen Kooperationsprojekte des Instituts mit Partnern aus Industrie und Wirtschaft.

Berichterstattung heißt hier Dokumentation darüber, wie aktuelle Ergebnisse aus mathematischer Forschungs- und Entwicklungsarbeit in industrielle Anwendungen und Softwareprodukte transferiert werden, und wie umgekehrt Probleme der Praxis neue interessante mathematische Fragestellungen generieren.

Prof. Dr. Dieter Prätzel-Wolters
Institutsleiter

Kaiserslautern, im Juni 2001

# IMRT planning on adaptive volume structures - a significant advance of computational complexity

**Alexander Scherrer[+], Karl-Heinz Küfer[+], Michael Monz[+], Fernando Alonso[+], Thomas Bortfeld[++]**

+: Department of Optimization, Fraunhofer Institut for Industrial Mathematics, Gottlieb-Daimler-Straße 49, 67663 Kaiserslautern, Germany
++: Department of Radiation Oncology, Massachusetts General Hospital and Harvard Medical School, 30 Fruit Street, Boston, MA 02114, USA

E-mail: scherrer,kuefer,monz,alonso@itwm.fhg.de, tbortfeld@partners.org

**Abstract.** In intensity-modulated radiotherapy (IMRT) planning the oncologist faces the challenging task of finding a treatment plan that he considers to be an ideal compromise of the inherently contradictive goals of delivering a sufficiently high dose to the target while widely sparing critical structures. The search for this a priori unknown compromise typically requires the computation of several plans, i.e. the solution of several optimization problems. This accumulates to a high computational expense due to the large scale of these problems - a consequence of the discrete problem formulation. This paper presents the *adaptive clustering method* as a new algorithmic concept to overcome these difficulties. The computations are performed on an individually adapted structure of voxel clusters rather than on the original voxels leading to a decisively reduced computational complexity as numerical examples on real clinical data demonstrate. In contrast to many other similar concepts, the typical tradeoff between a reduction in computational complexity and a loss in exactness can be avoided: the adaptive clustering method produces the optimum of the original problem. This flexible method can be applied to both single- and multi-criteria optimization methods based on most of the convex evaluation functions used in practice.

AMS classification scheme numbers: 65K05, 65M50, 65M55, 90C25,90C59, 90C90

Submitted to: *Physics in Medicine and Biology*

## 1. Introduction

In intensity-modulated radiotherapy (IMRT) planning the oncologist faces the challenging task of finding a treatment plan that he considers to be an ideal compromise of the inherently contradictive goals of delivering a sufficiently high dose to the target while widely sparing critical structures. The search for this a priori unknown compromise typically requires the computation of several plans, i.e. the solution of several optimization problems. This accumulates to a high computational expense due to the large scale of these problems - a consequence of the discrete problem formulation. An overview over the various aspects of IMRT is given in [Webb, 2001] and a description of the state-of-the-art and current research topics can be found in [IMRT Collaborative Working Group, 2001]. Some clinical aspects of IMRT can be found in [Zelefsky *et al.*, 2001, Pollack and Price, 2003, Chao and Blanco, 2003].
This paper presents the *adaptive clustering method* as a new algorithmic concept for the solution of such problems. The computations are performed on an individually adapted structure of voxel clusters rather than on the original voxels leading to a decisively reduced computational complexity. In contrast to many other similar concepts, the typical tradeoff between a reduction in computational complexity and a loss in exactness can be avoided: the adaptive clustering method produces the optimum of the original problem. Despite its original invention for the max and mean EUD model and a multi-criteria optimization concept, cf. [Thieke *et al.*, 2002, Küfer *et al.*, 2003], this flexible method can be applied to both single- and multi-criteria optimization methods based on most of the convex evaluation functions used in practice.
Starting with some modelling aspects of inverse treatment planning, a general formulation of the optimization problem is introduced. Then the principle and the perturbation aspects of clustering and the principle of problem adaptation by means of local refinement is introduced. These principle are then used for the construction of a hierarchical clustering and its utilization in a local refinement process, which yields the solution of the optimization problem.
The subsequent numerical examples on real clinical data give an impression of the practical performance of the method. The structure of the hierarchical clustering and the progress of the local refinement process are shown for a case of head and neck cancer. The second example, a case of prostate cancer, illustrates the geometrical shape of the cluster structures. Both examples contain a comparison of the CPU times required for a computation on the adaptive structures and for a straight-forward computation on the voxels, which demonstrates the high practical relevance of the adaptive clustering method.

### *1.1. The basic idea of the adaptive clustering method*

The optimization problem of IMRT treatment planning, i.e. the definition of its feasible region and formulation of the objective function(s) is based on the information about the dose distribution and its evaluation in the different structures (e.g. organs or artificial

entities) involved. Typically, the dose distribution attains an acceptable shape in most of the volume, such that the quality of a treatment plan strongly depends on the shape in some small volume parts, e.g. on the appearance of undesirable dose-volume effects. Roughly speaking, the dose distribution in these volume parts thus has to be carefully examined during the computation, whereas a short glance already suffices to obtain an acceptable result elsewhere. Therefore, not all details of the given information are really relevant to determine the optimal solution, i.e. only a very small part has to be known exactly whereas coarse knowledge without too much detail about the rest is already sufficient for the exact computation of the desired treatment plan. The adapted volume structure, i.e. the locally chosen shape and size of the voxel clusters represents these different resolutions of the information. The different levels of resolution to choose from are provided by the hierarchical clustering and the resolution, which is locally required for an exact computation of the optimum is determined during the local refinement process by a gradual increase in the refinement steps. This means, instead of a straightforward computation of the optimum based on the full amount of information, the adaptive clustering method performs the computation on a strongly simplified and thus much smaller amount of information, which is generated during the computation and still contains enough detail to yield the exact optimum.

## 2. Material and methods

### *2.1. The convex optimization problem*

*2.1.1. Basic notation* A treatment plan is physically determined by the irradiation geometry, which is assumed to be already given, and the intensity profile, i.e. the collection of intensity maps for the different beams. Let $B = \bigcup_i B_i$ denote the partition of the total beam area $B$ into the beam elements *bixels* and $V = \bigcup_j V_j$ the partition of the relevant part $V$ of the body volume into the volume elements *voxels*. We denote the space of intensity profiles, i.e. the vectors $\boldsymbol{x} = (x_i)$ containing the intensity values for the bixels $B_i$ of all beams, by $\mathcal{X}$. The realization of intensity maps with multileaf collimators or other devices, cf. [Webb, 1997], is not discussed in this paper. The dose distribution in the volume for an intensity profile $\boldsymbol{x}$ attains the form of a vector $\boldsymbol{D}(\boldsymbol{x}) = (\boldsymbol{D}_j(\boldsymbol{x}))$ with the dose values $\boldsymbol{D}_j(\boldsymbol{x}) = D(V_j)(\boldsymbol{x})$ in the voxels $V_j$. This dose vector follows as

$$\boldsymbol{D}(\boldsymbol{x}) = \boldsymbol{P} \cdot \boldsymbol{x}, \tag{1}$$

where the entry $\boldsymbol{P}_{j,i} = P(V_j, B_i)$ of the dose matrix $\boldsymbol{P}$ denotes the dose deposit of bixel $B_i$ into voxel $V_j$ by unit intensity. The entries of the j-th row vector $\boldsymbol{P_j}$ of the dose matrix denote the dose deposits of the different bixels $B_i$ into the corresponding voxel $V_j$ when radiating with unit intensity, hence the dose value for voxel $V_j$ follows as

$$\boldsymbol{D}_j(\boldsymbol{x}) = \boldsymbol{P_j} \cdot \boldsymbol{x}. \tag{2}$$

*2.1.2. Typical evaluation functions* The quality of a treatment plan with respect to an entity is evaluated by a function $F$ mapping the corresponding intensity vector $\boldsymbol{x} \in \mathcal{X}$

to a real value $F(\boldsymbol{x})$, i.e.

$$\begin{aligned} F : \mathcal{X} &\longrightarrow \mathbb{R}, \\ \boldsymbol{x} &\longmapsto F(\boldsymbol{x}). \end{aligned} \tag{3}$$

This function actually combines the computation of the dose distribution $\boldsymbol{D}(\boldsymbol{x})$ for an intensity vector $\boldsymbol{x}$ with its subsequent evaluation, which is no longer explicitly mentioned to ensure a simple notation.
There are different kinds of functions to evaluate a treatment plan in an entity, that measure, for example, deviations from a desired dose value $L_T$ in the target $T$ like

$$F_T(\boldsymbol{x}) = \max_{V_j \in T} |L_T - \boldsymbol{P_j} \cdot \boldsymbol{x}|, \tag{4}$$

or transgressions of an ideal upper dose bound $U_R$ in a critical structure $R$ like

$$F_R(\boldsymbol{x}) = \Big( \sum_{V_j \in R} (\boldsymbol{P_j} \cdot \boldsymbol{x} - U_R)_+^{\,p_R} \Big)^{\frac{1}{p_R}}, \quad p_R \in [1, \infty[. \tag{5}$$

Other functions take account of the whole shape of a dose distribution by means of an equivalent uniform dose (EUD), cf. e.g. [Brahme, 1984]. Using for example A. Niemierko's EUD, cf. [Niemierko, 1997], the deviation for the critical structure $R$ from a desirable upper bound $U_R$ is then measured by

$$F_R(\boldsymbol{x}) = \frac{1}{U_R} \Big( |R|^{-1} \sum_{V_j \in R} (\boldsymbol{P_j} \cdot \boldsymbol{x})^{p_R} \Big)^{\frac{1}{p_R}}, \quad p_R \in [1, \infty[, \tag{6}$$

where $|R|$ denotes the number of voxels in $R$.
The basic property of all such evalution functions is convexity.

*2.1.3. The optimization method* Based on the entity related evaluation functions, the optimization problem is formulated either in a single- or a multi-criteria way. Classical single-criteria approaches introduce a convex objective function by means of weighted scalarization, e.g.

$$F(\boldsymbol{x}) = \mu_T F_T(\boldsymbol{x}) + \mu_1 F_1(\boldsymbol{x}) + \ldots + \mu_K F_K(\boldsymbol{x}) \tag{7}$$

with some weight factors $\mu_T, \mu_1, \ldots \mu_K > 0$, where $F_T(\boldsymbol{x})$ denotes the evaluation function for the target and the $F_1(\boldsymbol{x}), \ldots F_K(\boldsymbol{x})$ denote the evaluation functions for the different critical structures, $R_1, \ldots R_K$. In modern multi-criteria approaches, cf. e.g. [Yu, 1997] and [Cotrutz *et al.*, 2001], the entity related functions enter as separate objective functions. Multi-criteria optimization can be done in many different ways, cf. e.g. [Steuer, 1985], that are all somehow based on a reasonably chosen reduction to a single-criteria optimization problem. In the single-criteria as well as the multi-criteria approach, some entities may also be excluded from the objective function(s) and enter the optimization problem as a convex hard constraint, e.g. like the target $T$ with

$$F_T(\boldsymbol{x}) =: L_T - \min_{V_j \in T} \boldsymbol{P_j} \cdot \boldsymbol{x} \leq 0 =: s_T, \tag{8}$$

with the strict lower dose bound $L_T$.

*2.1.4. The general problem formulation* All problems resulting from the different evaluation models and mathematical approaches above can thus be written in a general form with a convex feasible region denoted $\mathcal{X}_{feas} \subseteq \mathcal{X}$ as the set of all $\boldsymbol{x} \in \mathcal{X}$ that fulfill the involved hard constraints and a convex objective function $F(\boldsymbol{x})$ as

$$CP: \quad F(\boldsymbol{x}) \to \text{Min} \quad \text{subject to} \quad \boldsymbol{x} \in \mathcal{X}_{feas}. \tag{9}$$

To keep the notation simple, we restrict our theoretical considerations to the case of a single critical structure $R$, i.e. $F(\boldsymbol{x}) = F_R(\boldsymbol{x})$, and a single hard constraint (8) for the target, i.e.

$$\mathcal{X}_{feas}(s_T) = \{\boldsymbol{x} \in \mathcal{X}: \quad F_T(\boldsymbol{x}) \leq s_T\}. \tag{10}$$

Let

$$\mathcal{X}_{obj}(s) = \{\boldsymbol{x} \in \mathcal{X}: \quad F_R(\boldsymbol{x}) = s\} \tag{11}$$

denote the level set of all intensity vectors with an objective value $s$. The convex optimization problem (9) can then be rewritten as

$$CP: s \to \text{Min} \quad \text{subject to} \quad \mathcal{X}_{feas}(s_T) \cap \mathcal{X}_{obj}(s) \neq \emptyset. \tag{12}$$

The geometrical meaning of this formulation in the space $\mathcal{X}$ of all intensity maps is illustrated in figure 1, where each coordinate axis corresponds to one of the typically many hundred or several thousand bixels. $s^*$ is the smallest value, such that the corresponding level set $\mathcal{X}_{obj}(s^*)$ intersects the feasible region $\mathcal{X}_{feas}$. The typically non-unique optima $\boldsymbol{x}^*$ form the intersection

$$\mathcal{X}_{feas}(s_T) \cap \mathcal{X}_{obj}(s^*) = \{\boldsymbol{x} \in \mathcal{X}: \ \boldsymbol{x} \text{ optimum of } CP\}. \tag{13}$$

*2.2. The numerical expense of IMRT planning*

subsubsectionThe large scale situation
Evaluation of a treatment plan by one of the above mentioned functions $F(\boldsymbol{x})$ means evaluation of the previously computed dose distribution $\boldsymbol{D}(\boldsymbol{x})$ on the basis of the voxels that enter the $F(\boldsymbol{x})$ with their dose values (2). For example, the evaluation function (6) for the critical structure $R$ can be rewritten as

$$F_R(\boldsymbol{x}) = \Big( \sum_{V_j \in R} f_{V_j}(\boldsymbol{x}) \Big)^{\frac{1}{p_R}}, \quad f_{V_j}(\boldsymbol{x}) = \frac{1}{U_R^{p_R} \cdot |R|} \cdot (\boldsymbol{P_j} \cdot \boldsymbol{x})^{p_R}, \tag{14}$$

where the voxel related contributions $f_{V_j}(\boldsymbol{x})$ are based on the corresponding vectors $\boldsymbol{P_j}$. Typically, each of the several entities involved consists of several ten thousand or hundred thousand voxels, hence multiple computations of evaluation functions during the optimization are very expensive. This leads to a large scale problem (9) with a high computational complexity.
subsubsectionThe necessity for repeated plan computations

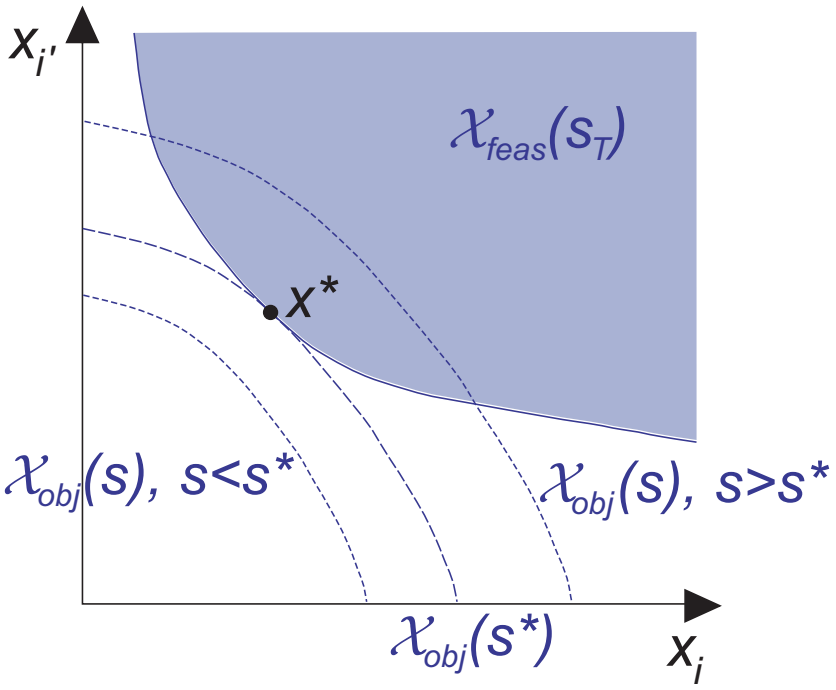


**Figure 1.** The set-based illustration of the optimization problem

Since the treatment possibilites of IMRT strongly depend on the specific clinical case and are thus not completely known at the beginning, the search for an optimal treatment plan typically requires the solution of several optimization problems in order to explore the limitations set by the introduced hard constraints and to study the remaining possibilities, e.g. the trade-off between different entity-related planning goals, cf. [Hunt *et al.*, 2002]. This is often done in a human iteration loop, where in each iterative step a plan is computed with the current objective function and, provided it does not satisfy all clinical goals, the evaluation function is modified for the next step, e.g. by modification of the weight vector in the single-criteria approach or some goal programming technique for the multi-criteria approach. Another option especially in the case of the multi-criteria approach is a precomputation of sufficiently many clinically reasonable plans in advance to choose from afterwards, cf. [Küfer *et al.*, 2000] and [Küfer *et al.*, 2003]. Combinations of these two main options that also share the need for repeated plan computations are also possible.

### *2.3. Hierarchical clustering and local refinement*

Up to now, reductions of the computational complexity of the problem (9) is typically obtained using simplified dose calculation algorithms or subsequent simplifications of the dose matrix, e.g. a sampling of matrix entries. This leads to simpler evaluation functions with approximate function values for all $\boldsymbol{x} \in \mathcal{X}$. In contrast to these approaches, the adaptive clustering method directly simplifies the evaluation functions in such a way,

that the optima $\boldsymbol{x}^*$ of (9) are still correctly valuated. The adaptive clustering method consists of two stages: first, a *hierarchical clustering method* provides a common data structure, which then serves as a "construction kit" for the *local refinement processes* performed in all future computations.
The voxels $V_j$ and their corresponding vectors $\boldsymbol{P_j}$ will form the basis, i.e. the 0-th level of the hierarchical clustering. To ensure a uniform notation, they are thus supplemented with an upper index (0), i.e. $V_j^{(0)}$ and $\boldsymbol{P_j}^{(0)}$.

*2.3.1. The clustering principle* Since the photon pencil beam is smooth due to scattering effects, the dose contribution from a bixel to voxels $V_\iota^{(0)}$ that are in the vicinity of each other is often quite similar. Hence the components of the vectors $\boldsymbol{P}_\iota^{(0)}$ of such voxels are similar. This can be exploited by merging such a family of neighbouring voxels belonging to the same entity to a cluster with a representative vector. The original voxel related contributions $f_{V_\iota^{(0)}}(\boldsymbol{x})$ can then be replaced by one single cluster related contribution $f_{V^{(1)}}(\boldsymbol{x})$. More precisely, let

$$\mathcal{C}^{(0)} := \{(V_\iota^{(0)}, \boldsymbol{P}_\iota^{(0)}) : \ \iota \in \mathcal{J}^{(0)}\} \tag{15}$$

denote the voxels with their corresponding vectors $\boldsymbol{P}_\iota^{(0)}$. Let $\{(V_\iota^{(0)}, \boldsymbol{P}_\iota^{(0)}) : \iota \in \mathcal{J}_j^{(0)}\}$, $\mathcal{J}_j^{(0)} \subset \mathcal{J}^{(0)}$ denote a family of voxels with similar $\boldsymbol{P}_\iota^{(0)}$. We merge the voxels of this family to a voxel cluster

$$V_j^{(1)} := \bigcup_{\iota \in \mathcal{J}_j^{(0)}} V_\iota^{(0)} \tag{16}$$

and form a representative vector

$$\boldsymbol{P_j}^{(1)} := \sum_{\iota \in \mathcal{J}_j^{(0)}} w_\iota^{(0)} \boldsymbol{P}_\iota^{(0)}, \quad w_\iota^{(0)} \geq 0 \tag{17}$$

by means of weighted aggregation. Altogether, we get a *cluster* $(V_j^{(1)}, \boldsymbol{P_j}^{(1)})$. If we apply this method to the whole volume $V$, we obtain a *clustering*

$$\mathcal{C}^{(1)} := \{(V_j^{(1)}, \boldsymbol{P_j}^{(1)}) : \ j \in \mathcal{J}^{(1)}\}, \quad \bigcup_{j \in \mathcal{J}^{(1)}} \mathcal{J}_j^{(0)} = \mathcal{J}^{(0)}, \tag{18}$$

cf. figure 3.
The weights $w_\iota^{(0)}$ in (17) are chosen in such a way, that the contributions $f_{V_\iota^{(0)}}(\boldsymbol{x})$ of the contained voxels to the evaluation function are well approximated by the contribution $f_{V_j^{(1)}}(\boldsymbol{x})$ of the cluster $V_j^{(1)}$. E.g. in the case of (14), for an equal weighting with

$$w_\iota^{(0)} \equiv |\mathcal{J}_j^{(0)}|^{\frac{1-p_R}{p_R}}, \quad \iota \in \mathcal{J}_j^{(0)}, \tag{19}$$

where $|\mathcal{J}_j^{(0)}|$ denotes the number of voxels in the cluster $V_j^{(1)}$, the cluster related error

$$\Delta f_{V_j^{(1)}}(\boldsymbol{x}) := \sum_{\iota \in \mathcal{J}_j^{(0)}} f_{V_\iota^{(0)}}(\boldsymbol{x}) - f_{V_j^{(1)}}(\boldsymbol{x}) \tag{20}$$

would be zero for a dose distribution that is constant in the cluster, thus rather small for dose distributions of low variation. The approximate evaluation function based on this clustering is then

$$F_R^{\mathcal{C}^{(1)}}(\boldsymbol{x}) = \Big( \sum_{j\in\mathcal{J}^{(1)}} f_{V_j^{(1)}}(\boldsymbol{x}) \Big)^{\frac{1}{p_R}} \tag{21}$$

$$= \underbrace{\Big( \sum_{\iota\in\mathcal{J}^{(0)}} f_{V_\iota^{(0)}}(\boldsymbol{x}) \Big)^{\frac{1}{p_R}}}_{=F_R^{\mathcal{C}^{(0)}}(\boldsymbol{x})} \cdot \left( 1 - \frac{\sum_{j\in\mathcal{J}^{(1)}} \Delta f_{V_j^{(1)}}(\boldsymbol{x})}{\sum_{\iota\in\mathcal{J}^{(0)}} f_{V_\iota^{(0)}}(\boldsymbol{x})} \right)^{\frac{1}{p_R}},$$

hence the evaluation error given by

$$\Delta F_R^{\mathcal{C}^{(1)}}(\boldsymbol{x}) := F_R^{\mathcal{C}^{(0)}}(\boldsymbol{x}) - F_R^{\mathcal{C}^{(1)}}(\boldsymbol{x}) \tag{22}$$

$$= F_R^{\mathcal{C}^{(0)}}(\boldsymbol{x}) \left[ 1 - \left( 1 - \frac{\sum_{j\in\mathcal{J}^{(1)}} \Delta f_{V_j^{(1)}}(\boldsymbol{x})}{\sum_{\iota\in\mathcal{J}^{(0)}} f_{V_\iota^{(0)}}(\boldsymbol{x})} \right)^{\frac{1}{p_R}} \right]$$

can be controlled by the cluster related errors (20).

**Conclusion:** *The clustering process, i.e. the transition from voxels to clusters turns the evaluation function into an approximate evaluation function, that can be computed with a much smaller expense at the cost of an only moderate evaluation error.*

*2.3.2. Perturbation aspects of the clustering* Since the optimization problem (12) is based on the evaluation functions, the transition to approximate functions also changes the problem itself. figure 2 illustrates the geometrical effect of the clustering on the level set $\mathcal{X}_{obj}(s^*)$. The perturbed set

$$\mathcal{X}_{obj}^{\mathcal{C}^{(1)}}(s^*) = \{\boldsymbol{x} \in \mathcal{X} : F_R^{\mathcal{C}^{(1)}}(\boldsymbol{x}) = s^*\} \tag{23}$$

and the original set

$$\mathcal{X}_{obj}^{\mathcal{C}^{(0)}}(s^*) = \{\boldsymbol{x} \in \mathcal{X} : F_R^{\mathcal{C}^{(0)}}(\boldsymbol{x}) = s^*\} \tag{24}$$

do not match exactly. This perturbation proceeds in the following way: consider an optimum $\boldsymbol{x}^* \in \mathcal{X}_{obj}^{\mathcal{C}^{(1)}}(s^*)$. The transition from voxels to clusters causes cluster related errors $\Delta f_{V_j^{(1)}}(\boldsymbol{x}^*)$, that accumulate to an evaluation error $\Delta F_R^{\mathcal{C}^{(1)}}(\boldsymbol{x}^*)$. Hence, the level set $\mathcal{X}_{obj}^{\mathcal{C}^{(0)}}(s^*)$ no longer passes through $\boldsymbol{x}^*$ itself, but passes somewhere nearby in some spatial distance depending on $\Delta F_R^{\mathcal{C}^{(1)}}(\boldsymbol{x}^*)$. Typically, the cluster related errors are very small for the vast majority of the clusters $V_j^{(1)}$, i.e.

$$|\Delta f_{V_j^{(1)}}(\boldsymbol{x}^*)| \leq \varepsilon \tag{25}$$

with some upper bound $\varepsilon > 0$, and thus contribute only marginally to the evaluation error $\Delta F_R^{\mathcal{C}^{(1)}}(\boldsymbol{x})$. Thus, the perturbation mainly traces back to the contributions of very few clusters located in a small volume part $\mathcal{V}(\boldsymbol{x}^*)$ of the critical structure $R$. Hence, the perturbation is of a local type:

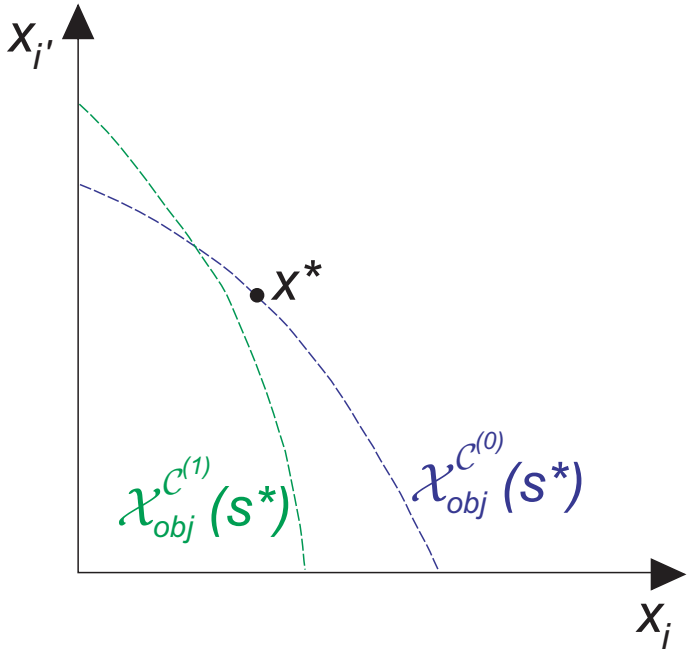


**Figure 2.** The original level set and its perturbation

there is a direct correspondence between the perturbation of some part of the set and the transition to clusters in a specific volume part.

**Conclusion:** *The transition from the original to the approximate evaluation functions perturbs the feasible region and the level sets of the optimization problem (1). The set perturbation proceeds locally, i.e. the perturbation of some part of a set corresponds to the transition from voxels to clusters in a local volume part.*

*2.3.3. Local approximation by means of adaptive clustering* According to the previous considerations, the evaluation error for $\boldsymbol{x}^*$ could thus be almost avoided by a transition from voxels to clusters only outside $\mathcal{V}(\boldsymbol{x}^*)$, for which $|\Delta f_{V_j^{(1)}}(\boldsymbol{x}^*)| \leq \varepsilon$, and using voxels inside $\mathcal{V}(\boldsymbol{x}^*)$. This combination $\mathcal{A} \subset \mathcal{C}^{(0)} \cup \mathcal{C}^{(1)}$ of voxels and clusters is called an *adaptive clustering*, cf. figure 3. According to (22), control (25) on the cluster related errors (20) also establishes control on the error of the adapted evaluation function $F_R^{\mathcal{A}}(\boldsymbol{x}^*)$ based on the adaptive clustering $\mathcal{A}$, i.e.

$$\Delta F_R^{\mathcal{A}}(\boldsymbol{x}^*) = F_R^{\mathcal{C}^{(0)}}(\boldsymbol{x}^*)\left[1-\left(1-\frac{\sum_{(V_j,\boldsymbol{P_j})\in\mathcal{A}\cup\mathcal{C}^{(1)}} \overbrace{\Delta f_{V_j}(\boldsymbol{x}^*)}^{|\cdot|\leq\varepsilon}}{\sum_{\iota\in\mathcal{J}^{(0)}} f_{V_\iota^{(0)}}(\boldsymbol{x}^*)}\right)^{\frac{1}{p_R}}\right] \overset{\varepsilon\to 0}{\longrightarrow} 0, \quad (26)$$

hence $\boldsymbol{x}^*$ itself and all neighbouring $\boldsymbol{x}$ are almost correctly evaluated by $F_R^{\mathcal{A}}(\boldsymbol{x})$. The effect on the level set is shown in figure 4: the boundaries of the original set (24) and the adapted set

$$\mathcal{X}_{obj}^{\mathcal{A}}(s^*) = \{\boldsymbol{x} \in \mathcal{X} : F_R^{\mathcal{A}}(\boldsymbol{x}) = s^*\} \quad (27)$$

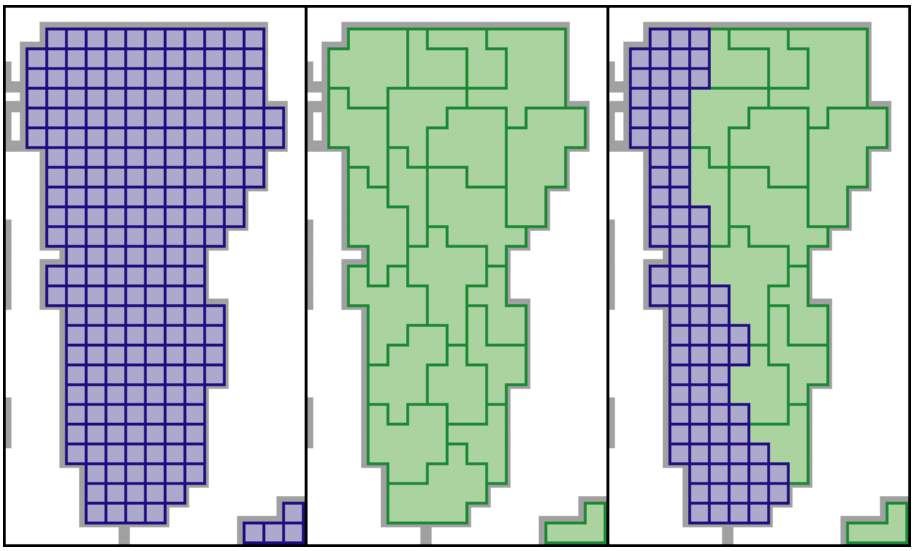

**Figure 3.** The different structures in the volume V consisting of the voxels (left) and the clusters (middle). An adaptive clustering (right) for $V$ consists of small voxels in $\mathcal{V}(\boldsymbol{x}^*)$ - here the left part of $V$ - and large clusters elsewhere.

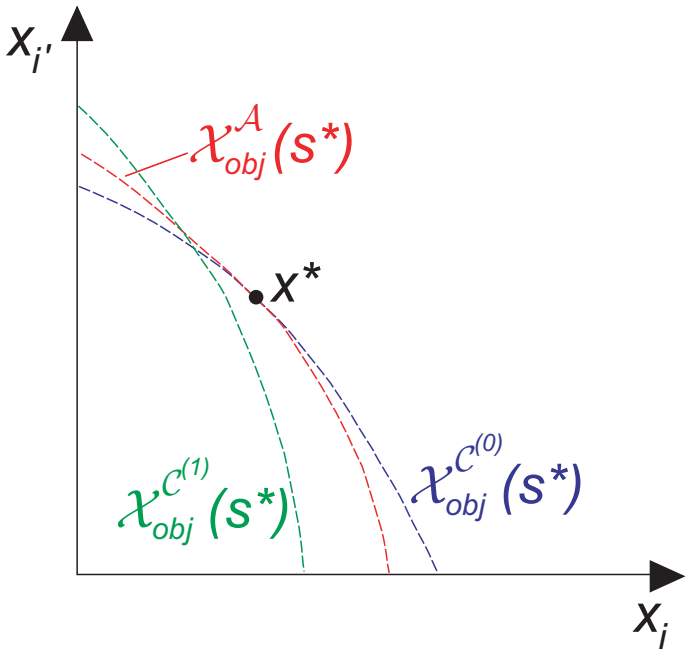


**Figure 4.** The local approximation of the level set

based on the adaptive clustering $\mathcal{A}$ match very well close to $\boldsymbol{x}^*$. Analogously, such a matching can also be obtained for the boundaries of the feasible regions, $bd\mathcal{X}^{\mathcal{A}}_{feas}(s_T)$ and $bd\mathcal{X}^{\mathcal{C}^{(0)}}_{feas}(s_T)$. This leads to the following conclusion: an adaptive clustering $\mathcal{A}$ for the target $T$ and the critical structure $R$ with the above mentioned properties implies

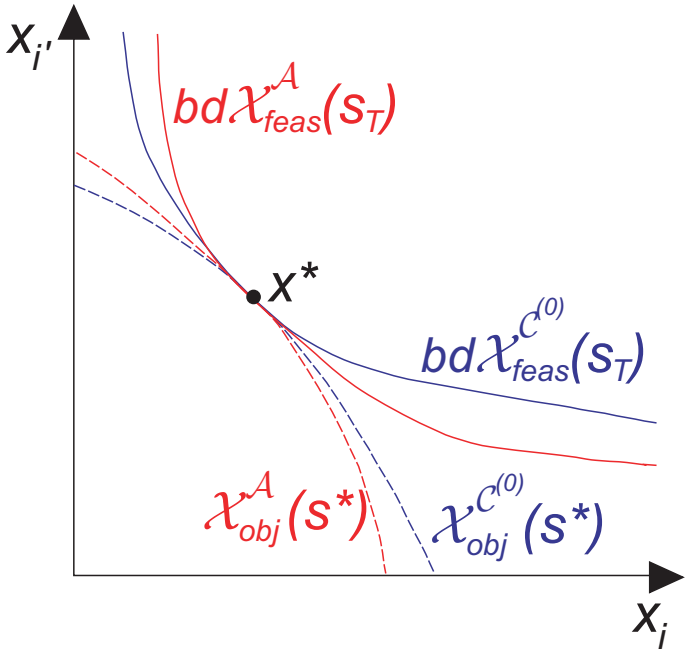


**Figure 5.** The original problem and an adapted problem

an adapted optimization problem

$$CP(\mathcal{A}) : s \to \text{Min} \qquad \text{subject to} \qquad \mathcal{X}^{(\mathcal{A})}_{feas}(s_T) \cap \mathcal{X}^{(\mathcal{A})}_{obj}(s) \neq \emptyset, \tag{28}$$

with a solution $s^*(\mathcal{A})$ and an optimum $\boldsymbol{x}^*(\mathcal{A})$, such that

$$\begin{aligned} s^*(\mathcal{A}) &= \min\{s \geq 0 : \mathcal{X}^{\mathcal{A}}_{feas}(s_T) \cap \mathcal{X}^{\mathcal{A}}_{obj}(s) \neq \emptyset\} \\ &= \min\{s \geq 0 : \mathcal{X}^{\mathcal{C}^{(0)}}_{feas}(s_T) \cap \mathcal{X}^{\mathcal{A}}_{obj}(s) \neq \emptyset\} \\ &= \min\{s \geq 0 : \mathcal{X}^{\mathcal{C}^{(0)}}_{feas}(s_T) \cap \mathcal{X}^{\mathcal{C}^{(0)}}_{obj}(s) \neq \emptyset\} = s^*, \end{aligned} \tag{29}$$

and thus

$$\boldsymbol{x}^*(\mathcal{A}) \in \mathcal{X}^{\mathcal{A}}_{feas}(s_T) \cap \mathcal{X}^{\mathcal{A}}_{obj}(s^*(\mathcal{A})) = \mathcal{X}^{\mathcal{C}^{(0)}}_{feas}(s_T) \cap \mathcal{X}^{\mathcal{C}^{(0)}}_{obj}(s^*), \tag{30}$$

cf. figure 5. Hence, $\boldsymbol{x}^*(\mathcal{A})$ is also an optimum of the original problem (12) according to (13), but its computation can be performed with a much smaller expense, since the number of volume elements $|\mathcal{A}|$ that have to be considered during the computation of $CP(\mathcal{A})$ is much smaller than the number of voxels $|\mathcal{C}^{(0)}|$ occuring in $CP(\mathcal{C})$.

**Conclusion:** *An adaptive clustering that avoids perturbations close to the optima of the original problem (12) by using voxels instead of clusters in some specific volume parts, implies an adapted optimization problem with the same optima that can be solved with a much smaller computational expense.*

*2.3.4. The local refinement principle* The exact location of $\boldsymbol{x}^*$ is not available, but can be approximately revealed by solving the approximate cluster-based optimization

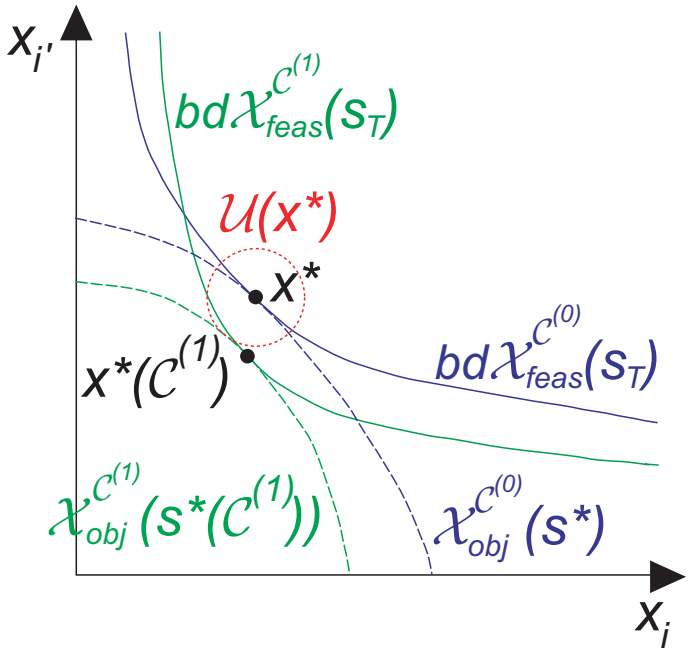


**Figure 6.** The solutions of the original and the approximate optimization problem

problem

$$CP(\mathcal{C}^{(1)}) : s \to \text{Min} \qquad \text{subject to} \qquad \mathcal{X}^{\mathcal{C}^{(1)}}_{feas}(s_T) \cap \mathcal{X}^{\mathcal{C}^{(1)}}_{obj}(s) \neq \emptyset. \tag{31}$$

that yields the solution $s^*(\mathcal{C}^{(1)})$ and an

$$\boldsymbol{x}^*(\mathcal{C}^{(1)}) \in \mathcal{X}^{\mathcal{C}^{(1)}}_{feas}(s_T) \cap \mathcal{X}^{\mathcal{C}^{(1)}}_{obj}(s^*(\mathcal{C}^{(1)})). \tag{32}$$

Since $\mathcal{X}^{\mathcal{C}^{(1)}}_{feas}(s_T)$ and $\mathcal{X}^{\mathcal{C}^{(1)}}_{obj}(s)$ are perturbations of $\mathcal{X}^{\mathcal{C}^{(0)}}_{feas}(s_T)$ and $\mathcal{X}^{\mathcal{C}^{(0)}}_{obj}(s)$,

$$\begin{aligned} s^*(\mathcal{C}^{(1)}) &= \min\{s \geq 0 : \mathcal{X}^{\mathcal{C}^{(1)}}_{feas}(s_T) \cap \mathcal{X}^{\mathcal{C}^{(1)}}_{obj}(s) \neq \emptyset\} \\ &\approx \min\{s \geq 0 : \mathcal{X}^{\mathcal{C}^{(0)}}_{feas}(s_T) \cap \mathcal{X}^{\mathcal{C}^{(1)}}_{obj}(s) \neq \emptyset\} \\ &\approx \min\{s \geq 0 : \mathcal{X}^{\mathcal{C}^{(0)}}_{feas}(s_T) \cap \mathcal{X}^{\mathcal{C}^{(0)}}_{obj}(s) \neq \emptyset\} = s^*, \end{aligned}$$

hence $\boldsymbol{x}^*(\mathcal{C}^{(1)})$ is quite close to $\boldsymbol{x}^* \in \mathcal{X}^{\mathcal{C}^{(0)}}_{feas}(s_T) \cap \mathcal{X}^{\mathcal{C}^{(0)}}_{obj}(s^*)$, cf. figure 6. The solution $\boldsymbol{x}^*(\mathcal{C}^{(1)})$ of $CP(\mathcal{C}^{(1)})$ thus reveals some set $\mathcal{U}(\boldsymbol{x}^*)$ containing $\boldsymbol{x}^*$. Analyzing the behaviour of the cluster related errors $\Delta f_{V_j^{(1)}}(\boldsymbol{x})$ reveals which clusters might exceed the upper error bound $\varepsilon$ in $\mathcal{U}(\boldsymbol{x}^*)$, i.e.

$$|\Delta f_{V_j^{(1)}}(\boldsymbol{x})| > \varepsilon \tag{33}$$

for some $\boldsymbol{x} \in \mathcal{U}(\boldsymbol{x}^*)$. This yields the desired information about the corresponding volume parts $\mathcal{V}_R(\mathcal{U}(\boldsymbol{x}^*)) \supseteq \mathcal{V}_R(\boldsymbol{x}^*)$ and $\mathcal{V}_T(\mathcal{U}(\boldsymbol{x}^*)) \supseteq \mathcal{V}_T(\boldsymbol{x}^*)$ in $R$ respectively $T$ in order to construct the adaptive clustering $\mathcal{A}$. This transition in some volume parts from the clusters back to the voxels is called *local refinement*.

**Conclusion:** *Solving the cluster-based problem (31) approximately reveals the location of the optima of the original problem (12). Based on this information, the adaptive clustering can then be constructed by a local refinement.*

*2.3.5. The hierarchical clustering method* In the most desirable situation, one would solve an approximate problem $CP(\mathcal{C}^{(1)})$ of very small computational complexity, i.e. a small number of large clusters, obtain precise information about the location of $\boldsymbol{x}^*$ in form of a small neighbourhood, then perform a local refinement in small volume parts, i.e. split up only a few clusters to obtain $\mathcal{A}$ and solve an adapted problem $CP(\mathcal{A})$ of only slightly increased computational complexity. However, this cannot be achieved: a small number of clusters in $\mathcal{C}^{(1)}$ imply large cluster related errors (20) and evaluation errors (22), causing a strong perturbation of the sets, hence a larger spatial distance between $\boldsymbol{x}^*(\mathcal{C}^{(1)})$ and $\boldsymbol{x}^*$ and a less accurate information about the location of $\boldsymbol{x}^*$, i.e. a larger set $\mathcal{U}(\boldsymbol{x}^*)$. On the other hand, a large number of clusters in $\mathcal{C}^{(1)}$ and $\mathcal{A}$ causes a high computational complexity of $CP(\mathcal{C}^{(1)})$ and $CP(\mathcal{A})$, hence the gain by solving two problems of moderate size instead of one large problem $CP(\mathcal{C}^{(0)})$ is not as large as desired. This drawback can be overcome by a refinement from the large clusters not directly down to the voxels, but to something 'in between'. This possiblity is provided by means of a *hierarchical clustering*.
Having constructed the clustering $\mathcal{C}^{(1)}$ of level 1 consisting of a comparably large number of rather small clusters, one continues iteratively by merging these clusters, resulting in the level 2-clustering $\mathcal{C}^{(2)}$, and so on up to some maximal level $l_{\max}$ with a desirably small number of large clusters. Strictly speaking, this iterative process yields a sequence of clusterings

$$\mathcal{C}^{(l)} := \{(V_j^{(l)}, \boldsymbol{P_j}^{(l)}) : \ j \in \mathcal{J}^{(l)}\}, \quad l = 0, \ldots, l_{\max} \tag{34}$$

where

$$\bigcup_{j \in \mathcal{J}^{(l+1)}} \mathcal{J}_j^{(l)} = \mathcal{J}^{(l)}, \quad V_j^{(l+1)} = \bigcup_{\iota \in \mathcal{J}_j^{(l)}} V_\iota^{(l)},$$
$$\boldsymbol{P_j}^{(l+1)} = \sum_{\iota \in \mathcal{J}_j^{(l)}} w_\iota^{(l)} \boldsymbol{P}_\iota^{(l)}, \quad w_\iota^{(l)} \geq 0.$$

The cluster related errors $\Delta f_{V_j^{(l)}}(\boldsymbol{x})$ and the evaluation error $\Delta F^{\mathcal{C}^{(l)}}(\boldsymbol{x})$, as defined in (20) and (22) increase with the level index $l$. These clusterings combine to a *hierarchical clustering* $\mathcal{C} := \bigcup_{l=0,\ldots,l_{\max}} \mathcal{C}^{(l)}$, cf. figures 7 and 8.

**Conclusion:** *The hierarchical clustering with its different clustering levels provides the additional possibilities needed for an adaptive clustering with moderately few elements that nevertheless yields an accurate problem approximation.*

*2.3.6. The local refinement process* The process starts with the coarsest possible clustering $\mathcal{A}^{(0)} := \mathcal{C}^{(l_{\max})} \subset \mathcal{C}$, i.e. the one of the highest level, with the corresponding

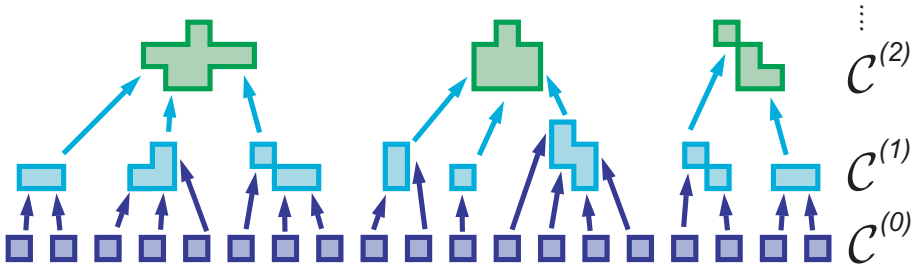


**Figure 7.** The level structure of the hierarchical clustering

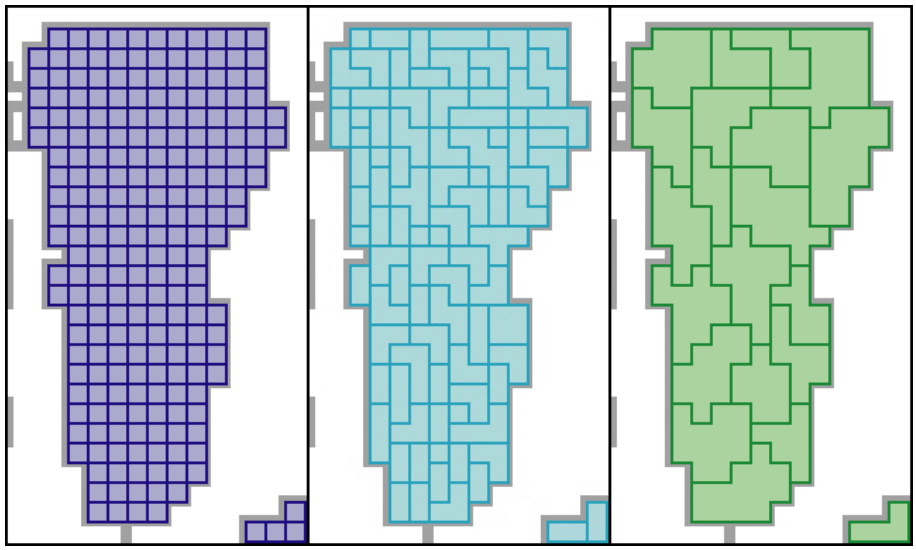

**Figure 8.** The levels 0 (left), 1 (middle) and 2 (right) of the hierarchical clustering in the volume $V$

approximate problem

$$CP(\mathcal{A}^{(0)}) : s \to \text{Min} \qquad \text{subject to}$$
$$\mathcal{X}_{feas}^{(\mathcal{A}^{(0)})}(s_T) \cap \mathcal{X}_{obj}^{(\mathcal{A}^{(0)})}(s) \neq \emptyset.$$

and obtains the solution $\boldsymbol{x}^*(\mathcal{A}^{(0)})$ as a first approximation of the original optimum $\boldsymbol{x}^*$. According to the local refinement principle, this solution reveals some information about the location of $\boldsymbol{x}^*$, which is rather coarse due to the small number of clusters in $\mathcal{A}^{(0)}$, i.e. $\mathcal{U}^{(0)}(\boldsymbol{x}^*)$ is quite large. Furthermore, since the cluster related errors $\Delta f_{V_j^{(l_{\max})}}(\boldsymbol{x})$ are large as already mentioned, many clusters will notably exceed the upper bound $\varepsilon$ in $\mathcal{U}^{(0)}(\boldsymbol{x}^*)$ leading to an unacceptably large number of candidates for the local refinement. Thus, a reasonably large error bound $\varepsilon^{(0)} > \varepsilon$ is introduced and the local refinement is performed only for those clusters that might exceed this bound in $\mathcal{U}^{(0)}(\boldsymbol{x}^*)$, i.e.

$$|\Delta f_{V_j^{(1)}}(\boldsymbol{x})| > \varepsilon^{(0)} \tag{35}$$

for an $\boldsymbol{x} \in \mathcal{U}^{(0)}(\boldsymbol{x}^*)$. These clusters are then split up into their subclusters of the next lower level to improve the control on the evaluation error, cf. (26). Together with

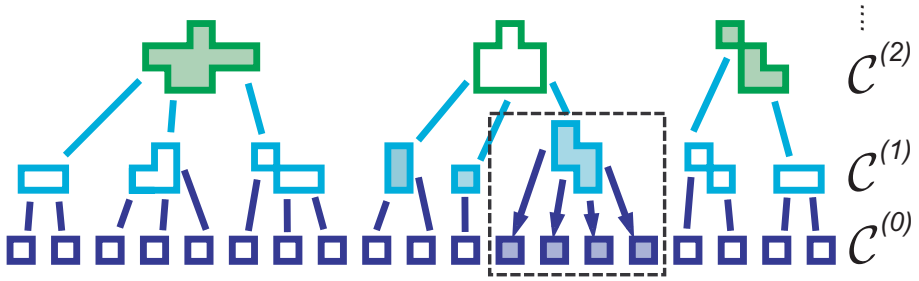


**Figure 9.** The refinement step from $\mathcal{A}^{(t)}$ to $\mathcal{A}^{(t+1)}$ in the hierarchical clustering

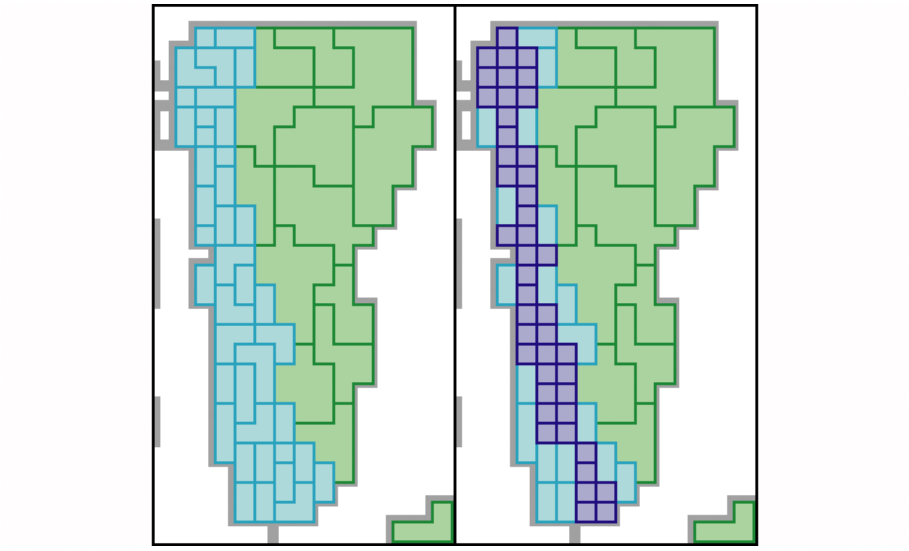

**Figure 10.** The refinement step from $\mathcal{A}^{(t)}$ (left) to $\mathcal{A}^{(t+1)}$ (right) in the volume $V$

the other retained clusters, these subclusters form the finer adaptive clustering $\mathcal{A}^{(1)}$ with an only moderately increased number of elements. The solution $\boldsymbol{x}^*(\mathcal{A}^{(1)})$ of the corresponding problem $CP(\mathcal{A}^{(1)})$ then provides more exact information about $\boldsymbol{x}^*$ in form of a typically smaller neighbourhood $\mathcal{U}^{(1)}(\boldsymbol{x}^*)$. The iterative continuation of this process, which is controlled by reasonably chosen error bounds

$$\varepsilon^{(t)}, \quad t = 0, 1, \ldots \tag{36}$$

with $\varepsilon^{(t)} > \varepsilon^{(t+1)}$, yields a series of adaptive clusterings

$$\mathcal{A}^{(t)} \subset \mathcal{C}, \quad t = 0, 1, \ldots \tag{37}$$

of increasing resolution with each refinement step being based on an analysis of the cluster related errors in $\mathcal{U}^{(t)}(\boldsymbol{x}^*)$, cf. figures 9 and 10, and the corresponding approximate problems

$$CP(\mathcal{A}^{(t)}) : s \to \text{Min} \qquad \text{subject to} \qquad \mathcal{X}_{feas}^{\mathcal{A}^{(t)}}(s_T) \cap \mathcal{X}_{obj}^{\mathcal{A}^{(t)}}(s) \neq \emptyset. \tag{38}$$

with the solutions $s^*(\mathcal{A}^{(t)})$ and $\boldsymbol{x}^*(\mathcal{A}^{(t)})$, cf. figure 11. This process terminates at some

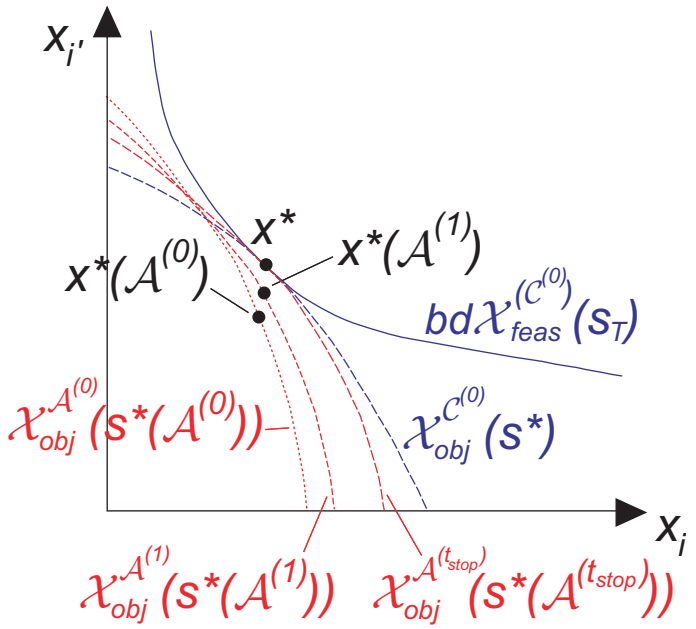


**Figure 11.** The geometrical illustration of the local refinement process

$t_{stop}$, where $\varepsilon^{(t_{stop})} = \varepsilon$, with an adaptive clustering $\mathcal{A}^{(t_{stop})}$ and a problem $CP(\mathcal{A}^{(t_{stop})})$, for which $s^*(\mathcal{A}^{(t_{stop})}) = s^*$ according to (29) and the optimum $\boldsymbol{x}^*(\mathcal{A}^{(t_{stop})})$ is an optimum of the original problem (12) according to (30).

**Conclusion:** *The local refinement process gradually reveals the location of the optima of the original problem (12) while keeping the number of elements in the adaptive clusterings $\mathcal{A}^{(t)}$ moderately low.*

*2.3.7. Complexity of the whole concept* Although the computation of $\boldsymbol{x}^*(t_{stop})$ requires the solution of the several approximate problems $CP(\mathcal{A}^{(0)}), \ldots, CP(\mathcal{A}^{(t_{stop})})$, the accumulated computational expense is still much smaller than the expense of a straightforward computation of (12) due to the fact that the number of clusters contained even in the largest adaptive clustering $\mathcal{A}^{(t_{stop})}$ is much smaller than the number of voxels in $\mathcal{C}^{(0)}$.

This leaves us with the computational expense for the hierarchical clustering method itself. It is performed only once in advance of the repeated plan computations, but the resulting hierarchical clustering then serves as a "construction kit" for the local refinement processes of all these computations. Its computational expense is rather small compared with the accumulated computational expense of the repeated computations, and in some cases, the method is even worthwhile performing for one single computation. One can even obtain a further reduction of the accumulated expense for the repeated plan computations, especially if these computations are performed iteratively as in current clinical practice (the situation is quite similar in case of a precomputation of plans). If the oncologist is not completely satisfied with the previously computed

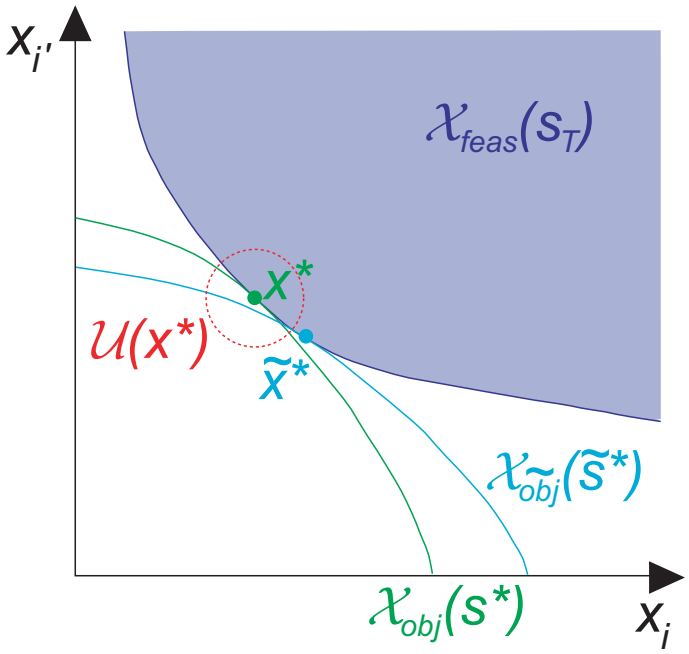


**Figure 12.** The optima $\boldsymbol{x}^*$ and $\tilde{\boldsymbol{x}}^*$ for the original and the modified objective function.

treatment plan and would like to modify some plan details in the subsequent computation, the objective function $F(\boldsymbol{x})$ is slightly modified to $\tilde{F}(\boldsymbol{x})$. The resulting plan $\tilde{\boldsymbol{x}}^*$ is then quite close to the old plan $\boldsymbol{x}^*$, cf. figure 12, and also close to or contained in a neighbourhood $\mathcal{U}(\boldsymbol{x}^*)$. The adapted clustering used for the computation of $\boldsymbol{x}^*$ is thus a very reasonable starting point for the computation of $\tilde{\boldsymbol{x}}^*$, cf. [Küfer *et al.*, 2003]. Quantitative results illustrating the significantly reduced computational expense are given for the subsequent examples on real clinical data.

### *2.4. Embedding the method in a general mathematical framework*

The adaptive clustering method method merges theoretically well-founded techniques from different fields of mathematics:
Clustering techniques originating from the wide field of classification, [IFCS, web site], are used in mathematical programming, cf. e.g. [Hansen and Jaumard, 1997], with a special focus on large scale handling by means of aggregation/disaggregation techniques [Evans *et al.*, 1991]. The continuous background of the discretized optimization problems occurring in IMRT planning allows an effective adaptation and extension of these techniques for the construction of the hierarchical clustering as a common "construction kit" for the computation of the several optimization problems that need to be solved.
In applied mathematics, the numerical solution of e.g. partial differential and integral equations is done by means of adaptive multigrid methods, cf. [Hackbusch, 2003]. Due to the continuous problem background, the concept of constructive grid adaptation can

be transferred to IMRT planning, whereas the regular grid structures are replaced by problem specific ones based on the previously constructed hierarchical clustering and the grid refinement proceeds within the structure of the hierarchy. Since the considered optimization problems are convex, the geometric aspect of the local refinement principle bears some resemblance to the approximation of convex sets known from convex analysis, cf. e.g. [Gruber, 1993].

## 3. Results and discussion

### *3.1. Numerical results on real clinical data*

The following numerical examples based on real clinical data were performed on a 1.7 GHz Pentium VI with 3 GB RAM to show the high practicability of the adaptive clustering method. Since the choice of evaluation functions und dose bounds is a very individual one, the problem formulation of the first example might not appeal to everyone. However, the magnitude of the computational complexity, which is our main interest, is not affected by this.

*3.1.1. Clinical example 1: a carcinoma in the head and neck region* The first clinical example is a carcinoma in the head and neck region. The cancerous tissue is classified into a boost volume and the surrounding remaining target volume. The critical structures involved are the adjacent myelon, brain stem and right parotis, furthermore the two eyes and the unclassified tissue. The irradiation geometry is a coplanar arrangement of seven equidistantly positioned beams with 1896 active bixels altogether, and the partition of the relevant body volume consists of 306742 voxels. The dose matrix contained 12.4% non-zero entries. The IMRT planning problem in this specific clinical case was modelled in the following way, whereas the dose bounds for the involved structures were chosen according to protocol RTOG H-0022, cf. [RTOG, web site]:
The condition on the minimum dose in the boost volume was set to

$$F_{B,L}(\boldsymbol{x}) := L_B - \min_{V_j \in B} \boldsymbol{P_j} \cdot \boldsymbol{x} \leq 0, \tag{39}$$

with $L_B = 72Gy$. The homogeneity condition entered with the evaluation function

$$F_{B,U}(\boldsymbol{x}) = \frac{\max_{V_j \in B} \boldsymbol{P_j} \cdot \boldsymbol{x}}{U_B} \tag{40}$$

and the ideal upper dose bound $L_U = 78Gy$. The target volume was treated analogously with $L_T = 66Gy$ and $L_U = 72Gy$. For the critical structures, account was taken on both the mean dose deposit and the local appearance of high dose values by means of the evaluation function

$$F_{R_k}(\boldsymbol{x}) = (1 - \alpha_k) \cdot \frac{1}{U_{R_k}} \Big( |R_k|^{-1} \sum_{V_j \in R_k} (\boldsymbol{P_j} \cdot \boldsymbol{x})^{p_{R_k}} \Big)^{\frac{1}{p_{R_k}}} \tag{41}$$

| Organ/Structure | $\lvert\mathcal{C}^{(0)}\rvert$ | $\lvert\mathcal{C}^{(1)}\rvert$ | $\lvert\mathcal{C}^{(2)}\rvert$ | $\lvert\mathcal{C}^{(3)}\rvert$ | ... | $\lvert\mathcal{C}^{(l_{\max})}\rvert$ |
|---|---|---|---|---|---|---|
| Boost | 13914 | 6957 | 1439 | 294 | | |
| Target | 42070 | 21035 | 5330 | 1424 | | |
| Myelon | 2346 | 1173 | 272 | 73 | | |
| Brain stem | 1200 | 600 | 134 | 38 | | |
| Right parotis | 1270 | 635 | 206 | 129 | ... | 101, $l_{\max} = 5$ |
| Right eye | 144 | 72 | 16 | | | |
| Left eye | 48 | 24 | 9 | | | |
| Unclassified tissue | 245750 | 122875 | 23384 | 4831 | ... | 286, $l_{\max} = 8$ |

**Table 1.** The number of levels and level related number of clusters of the hierarchical clustering

$$+ \ \alpha_k \cdot \frac{1}{V_{R_k}} \Big( |R_k|^{-1} \sum_{V_j \in R_k} (\boldsymbol{P_j} \cdot \boldsymbol{x})^{q_{R_k}} \Big)^{\frac{1}{q_{R_k}}}.$$

The first term with a comparably small $p_{R_k}$ and the ideal upper dose bound $U_{R_k}$ measures the mean dose, while the second term with larger $q_{R_k}$ and the ideal upper dose bound $V_{R_k}$ measures the tail of the dose distribution in the critical structure $R_k$. The parameter $\alpha_k \in [0, 1]$ determines whether there is more emphasis put on the mean dose of the tail. For the subsequent example, $U_{R_k} = V_{R_k}$ was set and the dose bounds and model parameters were chosen as

| Organ/Structure | $p_k$ | $q_k$ | $\alpha_k$ | $U_{R_k}$ |
|---|---|---|---|---|
| Myelon | 3.0 | 8.0 | 0.20 | 30 |
| Brain stem | 3.0 | 8.0 | 0.25 | 35 |
| Right parotis | 3.0 | 8.0 | 0.01 | 25 |
| Right eye | 3.0 | 8.0 | 0.30 | 10 |
| Left eye | 3.0 | 8.0 | 0.30 | 10 |
| Unclassified tissue | 1.1 | 3.0 | 0.99 | 15 |

At the common boundaries of boost and target and the unclassified tissue, the conditions on the dose distribution were slightly relaxed to steer the decay of dose deposits from the high values in boost and target to the low ones in the critical structures into a small volume passing along these boundaries with acceptably small dose volume effects. The optimization problem was formulated as

$$\begin{aligned} CP : s \to \text{Min} \qquad & \text{subject to} \\ & F_{B,L}(\boldsymbol{x}), F_{T,L}(\boldsymbol{x}) \leq 0, \\ & F_{B,U}(\boldsymbol{x}), F_{T,U}(\boldsymbol{x}), F_{R_k}(\boldsymbol{x}) \leq s. \end{aligned} \tag{42}$$

Concerning the hierarchical clustering method, the number of levels and level related number of clusters in the different entities are shown in table 1. For boost and target, the clustering process already stopped on level 3, since too large clusters would only increase the number of refinement steps required afterwards due to the minimal dose (39).

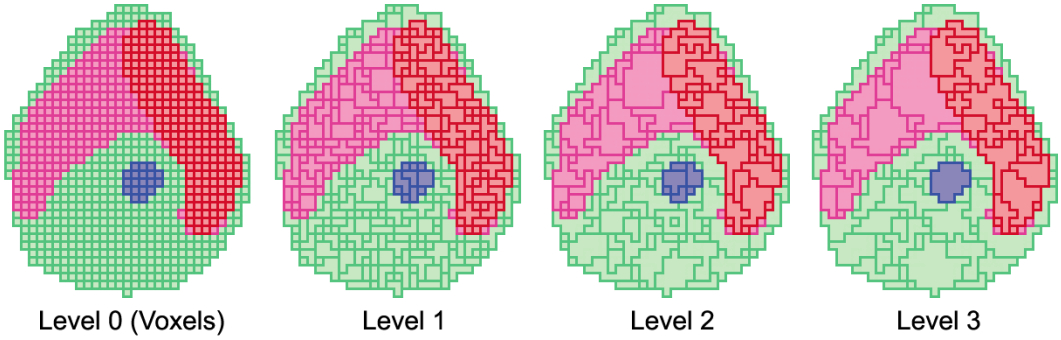


**Figure 13.** The clusterings $\mathcal{C}^{(l)}$ of the levels $l = 0, \ldots, 4$ in a transversal voxel layer. In this layer, the boost volume is located on the right side, the target on the left and the myelon in the centre. The remainder is the unclassified tissue.

| Organ/Structure | $\lvert\mathcal{A}^{(0)}\rvert$ | $\lvert\mathcal{A}^{(1)}\rvert$ | $\lvert\mathcal{A}^{(2)}\rvert$ | $\lvert\mathcal{A}^{(3)}\rvert$ | $\lvert\mathcal{A}^{(4)}\rvert$ |
|---|---|---|---|---|---|
| Boost | 294 | 1394 | 4456 | 4456 | 4456 |
| Target | 1424 | 4922 | 12928 | 12928 | 12928 |
| Myelon | 73 | 207 | 376 | 514 | 514 |
| Brain stem | 38 | 38 | 38 | 38 | 38 |
| Right parotis | 101 | 107 | 118 | 134 | 180 |
| Right eye | 16 | 16 | 16 | 16 | 16 |
| Left eye | 9 | 9 | 9 | 9 | 9 |
| Unclassified tissue | 286 | 383 | 383 | 383 | 383 |
| Whole volume | 2241 | 7076 | 18324 | 18478 | 18524 |

**Table 2.** The number of clusters of the adaptive clusterings contructed in the local refinement process

In the other entities, the method continued until the number of clusters was sufficiently small or the rate of reduction was too low. The proceeding of the hierarchical cluster method in a transversal voxel layer is shown in figure 13. The appearance of seemingly small clusters and single voxels even on high levels might be a bit misleading in view of the strongly reduced cluster numbers, but typically the clusters span over several layers containing only few voxels in each one. The refinement process took 5 steps to yield an optimum of the original problem with the number of clusters of the adaptive clusterings in the different entities given in table 2. Even the final and thus largest adaptive clustering $|\mathcal{A}^{(4)}|$ consisted of 18524 clusters, which is only 6.0% of the original number of 306742 voxels. The shape of these adaptive clusterings in the transversal voxel layer is shown in figure 14. The change of an intensity map for a single beam during the local refinement process as shown in figure 15 illustrates, how the approximate solutions approach the original solution $\boldsymbol{x}^*(\mathcal{A}^{(4)})$. Besides some minor modifications of fluence values especially on the left side of the intensity map, its general shape does not change.

It is self-evident, that the slight modifications of the intensity maps induce only minor

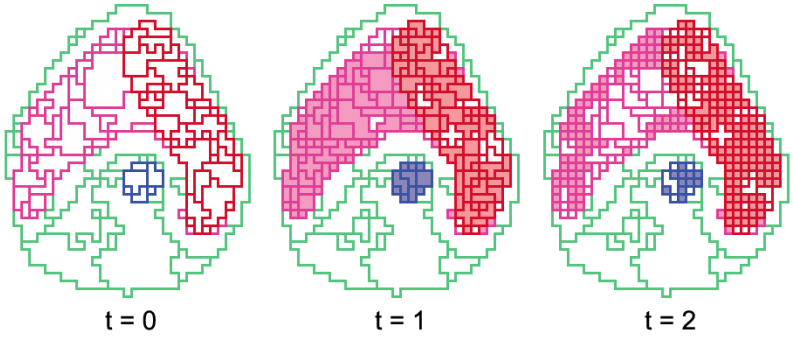


**Figure 14.** The refinement process and the adaptive clusterings $\mathcal{A}^{(t)}, t = 0, \ldots, 2$ in a transversal voxel layer. The further refinement steps do not alter the cluster structure in this layer. The filled clusters are the ones that were refined in the previous step. The refinements of some clusters happen in other layers and are thus not visible in the given one.

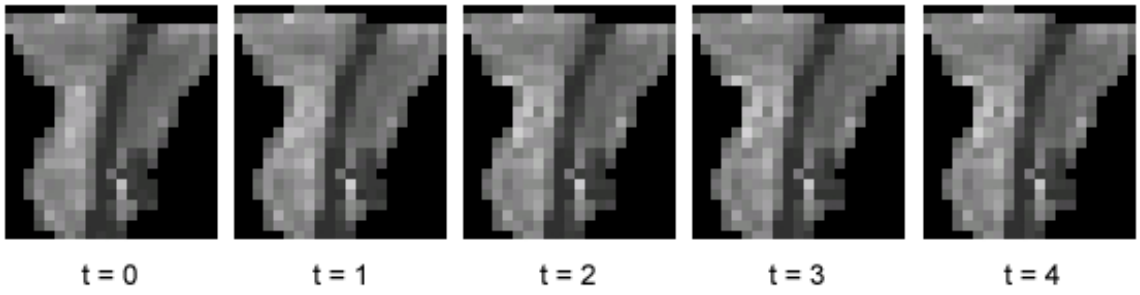


**Figure 15.** The intensity maps of $\boldsymbol{x}^*(t)$, $t = 0, \ldots, 4$ for one beam

changes of the dose-volume histograms for $\boldsymbol{x}^*(\mathcal{A}^{(t)})$, $t = 0, \ldots, 4$, cf. figure 16. As one can see, the dose-volume curves of the final solution $\boldsymbol{x}^*(\mathcal{A}^{(4)})$ all fulfill the RTOG H-0022 requirements.

The following CPU times give an impression about the computational complexity of the adaptive clustering method:
The hierarchical clustering method took 100 seconds and the optimization based on the local refinement process took 100 seconds, which is 19.0 % of the 525 seconds required for the straightforward computation on the voxels.

*3.1.2. Clinical example 2: a prostate carcinoma* The second clinical example is a case of a prostate carcinoma. Besides boost and target volume, the bladder, rectum, the two hips and the unclassified tissue are involved, cf. figure (17,left). The irradiation geometry is a coplanar arrangement of five equidistantly located beams with 400 active bixels altogether, and the partition of the relevant body volume consists of 435501 voxels. The dose matrix contained 12.0% non-zero entries. This case is well suited to demonstrate how the construction of the clusters performs. figure (17,right) shows the

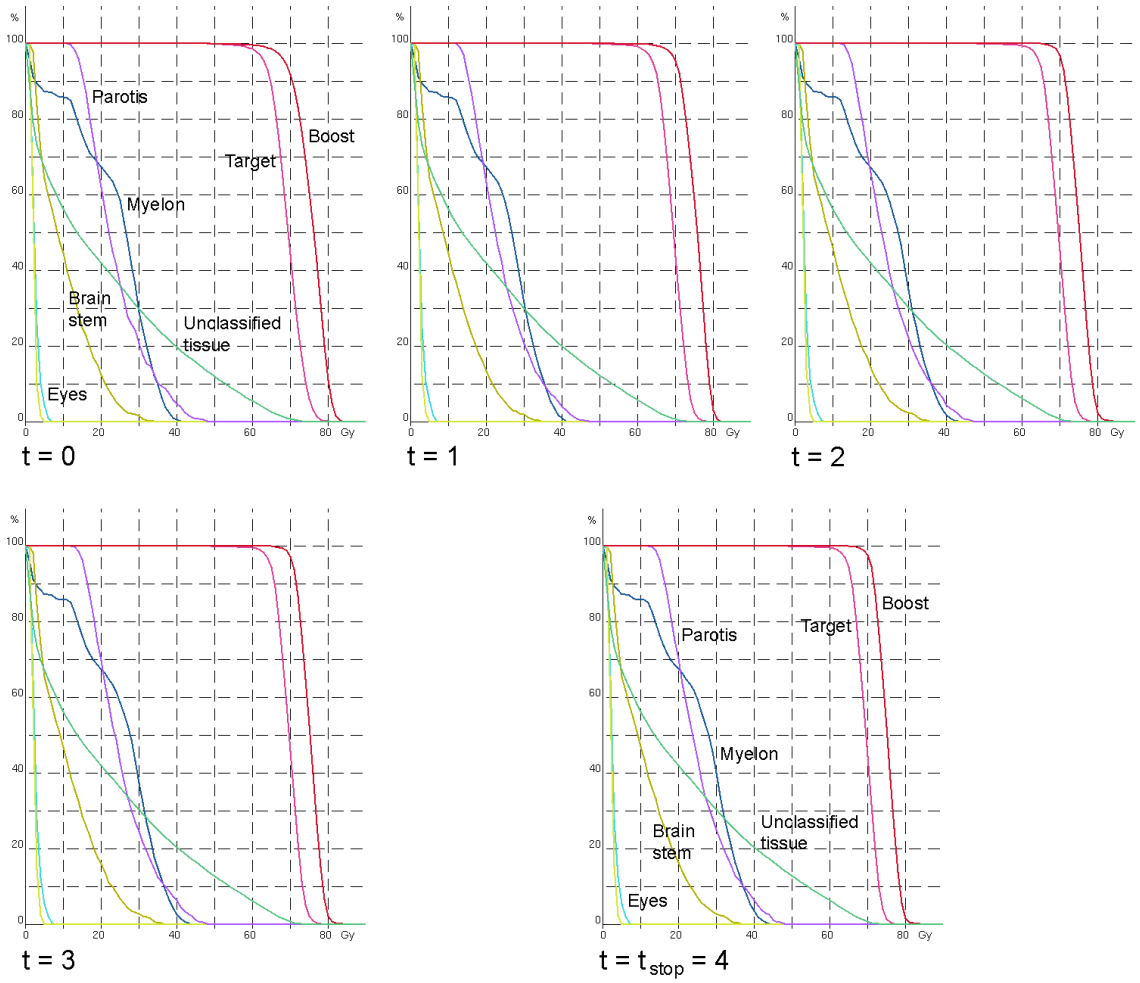


**Figure 16.** The dose-volume histograms of $\boldsymbol{x}^*(\mathcal{A}^{(t)})$, $t = 0, \ldots, 4$

clustering $|\mathcal{C}^{(3)}|$ of an upper level in the transversal voxel layer through the isocentre. Comparison with figure (17,left) illustrates that the shapes of the clusters well represent the irradiation geometry, i.e. they pass along the beam directions.
The hierarchical clustering contained 3-8 levels depending on the organ. The refinement process terminated after 2 steps with an adaptive clustering consisting of 4369 clusters, which is 1% of the original number of voxels. Performing the adaptive clustering method in the special case required 83 seconds CPU time for the hierarchical clustering method and 11 seconds CPU time for the optimization based on the local refinement process, which is only 2.7% of the 403 seconds needed for the straightforward computation on the voxels.

## 4. Conclusion

The presented adaptive clustering method leads to a decisive speed-up in plan computation allowing a more efficient use of the limited time that is available in IMRT

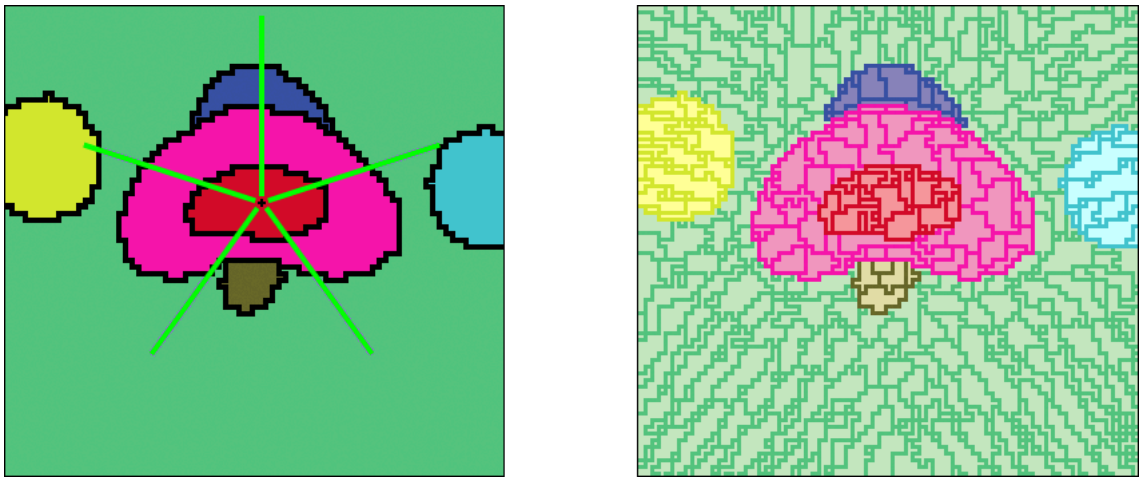

**Figure 17.** Left hand side: The organ geometry with boost and target (centre), the adjacent bladder (above target) and rectum (below target) and the two hips. The lines heading towards the isocentre (cross in the centre) visualize the beam directions.
Right hand side: The clustering structure on level 3, which well represents the beam directions.

treatment planning to find a desirable therapy. Possible extensions of this flexible method to several other questions in the field of IMRT treatment planning, e.g. an fast plan adaptation to a changed organ geometry or the integration of the sequencing, i.e. the generation of fitting aperture arrangements for the beams into the plan computation are future research topics.

## Acknowledgments

The authors are grateful to the members of the Department of Medical Physics in Radiation Oncology of Wolfgang Schlegel and the Clinical Cooperation Unit Radiation Oncology of Jürgen Debus at the German Cancer Research Center (DKFZ), Heidelberg (Germany), for a successful scientific cooperation. Special thanks are adressed to Christian Thieke and Uwe Oelfke for a long lasting teamwork and to Christoph Thilmann for the helpful consulting in clinical questions.

## References

[Brahme, 1984] Anders Brahme. Dosimetric precision requirements in radiation therapy. *Acta Radiologica - Oncology*, 23:379–391, 1984.

[Chao and Blanco, 2003] K. S. Clifford Chao and Angel I. Blanco. Intensity-modulated radiation therapy for head and neck cancer. In Jatinder R. Palta and T. Rockwell Mackie, editors, *Intensity-modulated radiation therapy: the state of the art*, pages 631–644. Medical Physics Publishing, 2003.

[Cotrutz *et al.*, 2001] Cristian Cotrutz, Michael Lahanas, Kostas Kappas, and Dimos Baltas. A multiobjective gradient based dose optimization algorithm for external beam conformal radiotherapy. *Physics in Medicine and Biology*, 46:2161–2175, 2001.

[Evans *et al.*, 1991] James Evans, Robert D. Plante, David F. Rogers, and Richard T. Wong. Aggregation and disaggregation techniques and methodology in optimization. *Operations Research*, 39(4):553–582, 1991.

[Gruber, 1993] Peter M. Gruber, editor. *Handbook of Convex Geometry*. Elsevier Science Publishers, 1993.

[Hackbusch, 2003] Wolfgang Hackbusch. *Multi-Grid Methods and Applications*. Springer-Verlag, Berlin, 2003.

[Hansen and Jaumard, 1997] Pierre Hansen and Brigitte Jaumard. Cluster analysis and mathematical programming. *Mathematical Programming*, 79:191–215, 1997.

[Hunt *et al.*, 2002] Margie A. Hunt, Ching-Yeh Hsiung, Spiridon V. Spirou, Chen-Shou Chui, Howard I. Amols, and Clifton C. Ling. Evaluation of concave dose distributions created using an inverse planning system. *International Journal of Radioation Oncology, Biology, Physics*, 54(3):953–962, 2002.

[IFCS, web site] International Federation of Classification Societies IFCS. *http://www.classification-society.org/*, web site.

[IMRT Collaborative Working Group, 2001] IMRT Collaborative Working Group. Intensity-modulated radiotherapy: current status and issues of interest. *International Journal of Radioation Oncology, Biology, Physics*, 51(4):880–914, 2001.

[Küfer *et al.*, 2000] Karl-Heinz Küfer, Horst W. Hamacher, and Thomas R. Bortfeld. A multicriteria optimization approach for inverse radiotherapy planning. In Thmoas R. Bortfeld and Wolfgang Schlegel, editors, *Proceedings of the XIIIth ICCR, Heidelberg 2000*, pages 26–29, 2000.

[Küfer *et al.*, 2003] Karl-Heinz Küfer, Alexander Scherrer, Michael Monz, Fernando Alonso, Hans Trinkaus, Thomas Bortfeld, and Christian Thieke. Intensity-modulated radiotherapy - a large scale multi-criteria programming problem. *OR Spectrum*, 25:223–249, 2003.

[Niemierko, 1997] Andrzej Niemierko. Reporting and analysing dose distributions: a concept of equivalent uniform dose. *Medical Physics*, 24:103–110, 1997.

[Pollack and Price, 2003] Alan Pollack and Robert A. Price. Imrt for prostate cancer. In Jatinder R. Palta and T. Rockwell Mackie, editors, *Intensity-modulated radiation therapy: the state of the art*, pages 617–630. Medical Physics Publishing, 2003.

[RTOG, web site] Radiation Therapy Oncology Group RTOG. *http://www.rtog.org/*, web site.

[Steuer, 1985] Ralph E. Steuer. *Multicriteria Optimization: Theory, Computation and Applications*. Wiley, NewYork, 1985.

[Thieke *et al.*, 2002] Christian Thieke, Thomas Bortfeld, and Karl-Heinz Küfer. Characterization of dose distributions through the max and mean dose concept. *Acta Oncologica*, 41:158–161, 2002.

[Webb, 1997] Steve Webb. *The physics of conformal radiotherapy - advances in technology*. Medical Science Series. Institute of Physics Publishing, Bristol and Philadelphia, 1997.

[Webb, 2001] Steve Webb. *Intensity-modulated radiation therapy*. Series in Medical Physics. Institute of Physics Publishing, Bristol and Philadelphia, 2001.

[Yu, 1997] Yan Yu. Multiobjective decision theory for computational optimization in radiation therapy. *Medical Physics*, 24:1445–1454, 1997.

[Zelefsky *et al.*, 2001] Michael J. Zelefsky, Zvi Fuks, Margie A. Hunt, Yoshiya Yamada, C. Marion, C. Clifton Ling, H. Amols, Ennapadam S. Venkatraman, and Stephen A. Leibel. High-dose intensity modulated radiation therapy for prostate cancer: early toxicity and biochemical outcome in 772 patients. *International Journal of Radioation Oncology, Biology, Physics*, 53(5):1111–1116, 2001.

# Published reports of the Fraunhofer ITWM

The PDF-files of the following reports are available under:
*www.itwm.fraunhofer.de/rd/presse/berichte*

1. D. Hietel, K. Steiner, J. Struckmeier

***A Finite - Volume Particle Method for Compressible Flows***

We derive a new class of particle methods for conservation laws, which are based on numerical flux functions to model the interactions between moving particles. The derivation is similar to that of classical Finite-Volume methods; except that the fixed grid structure in the Finite-Volume method is substituted by so-called mass packets of particles. We give some numerical results on a shock wave solution for Burgers equation as well as the well-known one-dimensional shock tube problem.
(19 pages, 1998)

2. M. Feldmann, S. Seibold

***Damage Diagnosis of Rotors: Application of Hilbert Transform and Multi-Hypothesis Testing***

In this paper, a combined approach to damage diagnosis of rotors is proposed. The intention is to employ signal-based as well as model-based procedures for an improved detection of size and location of the damage. In a first step, Hilbert transform signal processing techniques allow for a computation of the signal envelope and the instantaneous frequency, so that various types of non-linearities due to a damage may be identified and classified based on measured response data. In a second step, a multi-hypothesis bank of Kalman Filters is employed for the detection of the size and location of the damage based on the information of the type of damage provided by the results of the Hilbert transform.
*Keywords: Hilbert transform, damage diagnosis, Kalman filtering, non-linear dynamics*
(23 pages, 1998)

3. Y. Ben-Haim, S. Seibold

***Robust Reliability of Diagnostic Multi-Hypothesis Algorithms: Application to Rotating Machinery***

Damage diagnosis based on a bank of Kalman filters, each one conditioned on a specific hypothesized system condition, is a well recognized and powerful diagnostic tool. This multi-hypothesis approach can be applied to a wide range of damage conditions. In this paper, we will focus on the diagnosis of cracks in rotating machinery. The question we address is: how to optimize the multi-hypothesis algorithm with respect to the uncertainty of the spatial form and location of cracks and their resulting dynamic effects. First, we formulate a measure of the reliability of the diagnostic algorithm, and then we discuss modifications of the diagnostic algorithm for the maximization of the reliability. The reliability of a diagnostic algorithm is measured by the amount of uncertainty consistent with no-failure of the diagnosis. Uncertainty is quantitatively represented with convex models.
*Keywords: Robust reliability, convex models, Kalman filtering, multi-hypothesis diagnosis, rotating machinery, crack diagnosis*
(24 pages, 1998)

4. F.-Th. Lentes, N. Siedow

***Three-dimensional Radiative Heat Transfer in Glass Cooling Processes***

For the numerical simulation of 3D radiative heat transfer in glasses and glass melts, practically applicable mathematical methods are needed to handle such problems optimal using workstation class computers. Since the exact solution would require super-computer capabilities we concentrate on approximate solutions with a high degree of accuracy. The following approaches are studied: 3D diffusion approximations and 3D ray-tracing methods.
(23 pages, 1998)

5. A. Klar, R. Wegener

***A hierarchy of models for multilane vehicular traffic***
***Part I: Modeling***

In the present paper multilane models for vehicular traffic are considered. A microscopic multilane model based on reaction thresholds is developed. Based on this model an Enskog like kinetic model is developed. In particular, care is taken to incorporate the correlations between the vehicles. From the kinetic model a fluid dynamic model is derived. The macroscopic coefficients are deduced from the underlying kinetic model. Numerical simulations are presented for all three levels of description in [10]. Moreover, a comparison of the results is given there.
(23 pages, 1998)

***Part II: Numerical and stochastic investigations***

In this paper the work presented in [6] is continued. The present paper contains detailed numerical investigations of the models developed there. A numerical method to treat the kinetic equations obtained in [6] are presented and results of the simulations are shown. Moreover, the stochastic correlation model used in [6] is described and investigated in more detail.
(17 pages, 1998)

6. A. Klar, N. Siedow

***Boundary Layers and Domain Decomposition for Radiative Heat Transfer and Diffusion Equations: Applications to Glass Manufacturing Processes***

In this paper domain decomposition methods for radiative transfer problems including conductive heat transfer are treated. The paper focuses on semi-transparent materials, like glass, and the associated conditions at the interface between the materials. Using asymptotic analysis we derive conditions for the coupling of the radiative transfer equations and a diffusion approximation. Several test cases are treated and a problem appearing in glass manufacturing processes is computed. The results clearly show the advantages of a domain decomposition approach. Accuracy equivalent to the solution of the global radiative transfer solution is achieved, whereas computation time is strongly reduced.
(24 pages, 1998)

7. I. Choquet

***Heterogeneous catalysis modelling and numerical simulation in rarified gas flows Part I: Coverage locally at equilibrium***

A new approach is proposed to model and simulate numerically heterogeneous catalysis in rarefied gas flows. It is developed to satisfy all together the following points:
1) describe the gas phase at the microscopic scale, as required in rarefied flows,
2) describe the wall at the macroscopic scale, to avoid prohibitive computational costs and consider not only crystalline but also amorphous surfaces,
3) reproduce on average macroscopic laws correlated with experimental results and
4) derive analytic models in a systematic and exact way. The problem is stated in the general framework of a non static flow in the vicinity of a catalytic and non porous surface (without aging). It is shown that the exact and systematic resolution method based on the Laplace transform, introduced previously by the author to model collisions in the gas phase, can be extended to the present problem. The proposed approach is applied to the modelling of the EleyRideal and LangmuirHinshelwood recombinations, assuming that the coverage is locally at equilibrium. The models are developed considering one atomic species and extended to the general case of several atomic species. Numerical calculations show that the models derived in this way reproduce with accuracy behaviors observed experimentally.
(24 pages, 1998)

8. J. Ohser, B. Steinbach, C. Lang

***Efficient Texture Analysis of Binary Images***

A new method of determining some characteristics of binary images is proposed based on a special linear filtering. This technique enables the estimation of the area fraction, the specific line length, and the specific integral of curvature. Furthermore, the specific length of the total projection is obtained, which gives detailed information about the texture of the image. The influence of lateral and directional resolution depending on the size of the applied filter mask is discussed in detail. The technique includes a method of increasing directional resolution for texture analysis while keeping lateral resolution as high as possible.
(17 pages, 1998)

9. J. Orlik

***Homogenization for viscoelasticity of the integral type with aging and shrinkage***

A multiphase composite with periodic distributed inclusions with a smooth boundary is considered in this contribution. The composite component materials are supposed to be linear viscoelastic and aging (of the nonconvolution integral type, for which the Laplace transform with respect to time is not effectively applicable) and are subjected to isotropic shrinkage. The free shrinkage deformation can be considered as a fictitious temperature deformation in the behavior law. The procedure presented in this paper proposes a way to determine average (effective homogenized) viscoelastic and shrinkage (temperature) composite properties and the homogenized stressfield from known properties of the components. This is done by the extension of the asymptotic homogenization technique known for pure elastic nonhomogeneous bodies to the nonhomogeneous thermoviscoelasticity of the integral noncon-

volution type. Up to now, the homogenization theory has not covered viscoelasticity of the integral type. SanchezPalencia (1980), Francfort & Suquet (1987) (see [2], [9]) have considered homogenization for viscoelasticity of the differential form and only up to the first derivative order. The integralmodeled viscoelasticity is more general then the differential one and includes almost all known differential models. The homogenization procedure is based on the construction of an asymptotic solution with respect to a period of the composite structure. This reduces the original problem to some auxiliary boundary value problems of elasticity and viscoelasticity on the unit periodic cell, of the same type as the original non-homogeneous problem. The existence and uniqueness results for such problems were obtained for kernels satisfying some constrain conditions. This is done by the extension of the Volterra integral operator theory to the Volterra operators with respect to the time, whose 1 kernels are space linear operators for any fixed time variables. Some ideas of such approach were proposed in [11] and [12], where the Volterra operators with kernels depending additionally on parameter were considered. This manuscript delivers results of the same nature for the case of the spaceoperator kernels.
(20 pages, 1998)

10. J. Mohring

***Helmholtz Resonators with Large Aperture***

The lowest resonant frequency of a cavity resonator is usually approximated by the classical Helmholtz formula. However, if the opening is rather large and the front wall is narrow this formula is no longer valid. Here we present a correction which is of third order in the ratio of the diameters of aperture and cavity. In addition to the high accuracy it allows to estimate the damping due to radiation. The result is found by applying the method of matched asymptotic expansions. The correction contains form factors describing the shapes of opening and cavity. They are computed for a number of standard geometries. Results are compared with numerical computations.
(21 pages, 1998)

11. H. W. Hamacher, A. Schöbel

***On Center Cycles in Grid Graphs***

Finding "good" cycles in graphs is a problem of great interest in graph theory as well as in locational analysis. We show that the center and median problems are NP hard in general graphs. This result holds both for the variable cardinality case (i.e. all cycles of the graph are considered) and the fixed cardinality case (i.e. only cycles with a given cardinality p are feasible). Hence it is of interest to investigate special cases where the problem is solvable in polynomial time. In grid graphs, the variable cardinality case is, for instance, trivially solvable if the shape of the cycle can be chosen freely. If the shape is fixed to be a rectangle one can analyze rectangles in grid graphs with, in sequence, fixed dimension, fixed cardinality, and variable cardinality. In all cases a complete characterization of the optimal cycles and closed form expressions of the optimal objective values are given, yielding polynomial time algorithms for all cases of center rectangle problems. Finally, it is shown that center cycles can be chosen as rectangles for small cardinalities such that the center cycle problem in grid graphs is in these cases completely solved.
(15 pages, 1998)

12. H. W. Hamacher, K.-H. Küfer

***Inverse radiation therapy planning - a multiple objective optimisation approach***

For some decades radiation therapy has been proved successful in cancer treatment. It is the major task of clinical radiation treatment planning to realize on the one hand a high level dose of radiation in the cancer tissue in order to obtain maximum tumor control. On the other hand it is obvious that it is absolutely necessary to keep in the tissue outside the tumor, particularly in organs at risk, the unavoidable radiation as low as possible.
No doubt, these two objectives of treatment planning - high level dose in the tumor, low radiation outside the tumor - have a basically contradictory nature. Therefore, it is no surprise that inverse mathematical models with dose distribution bounds tend to be infeasible in most cases. Thus, there is need for approximations compromising between overdosing the organs at risk and underdosing the target volume.
Differing from the currently used time consuming iterative approach, which measures deviation from an ideal (non-achievable) treatment plan using recursively trial-and-error weights for the organs of interest, we go a new way trying to avoid a priori weight choices and consider the treatment planning problem as a multiple objective linear programming problem: with each organ of interest, target tissue as well as organs at risk, we associate an objective function measuring the maximal deviation from the prescribed doses.
We build up a data base of relatively few efficient solutions representing and approximating the variety of Pareto solutions of the multiple objective linear programming problem. This data base can be easily scanned by physicians looking for an adequate treatment plan with the aid of an appropriate online tool.
(14 pages, 1999)

13. C. Lang, J. Ohser, R. Hilfer

***On the Analysis of Spatial Binary Images***

This paper deals with the characterization of microscopically heterogeneous, but macroscopically homogeneous spatial structures. A new method is presented which is strictly based on integral-geometric formulae such as Crofton's intersection formulae and Hadwiger's recursive definition of the Euler number. The corresponding algorithms have clear advantages over other techniques. As an example of application we consider the analysis of spatial digital images produced by means of Computer Assisted Tomography.
(20 pages, 1999)

14. M. Junk

***On the Construction of Discrete Equilibrium Distributions for Kinetic Schemes***

A general approach to the construction of discrete equilibrium distributions is presented. Such distribution functions can be used to set up Kinetic Schemes as well as Lattice Boltzmann methods. The general principles are also applied to the construction of Chapman Enskog distributions which are used in Kinetic Schemes for compressible Navier-Stokes equations.
(24 pages, 1999)

15. M. Junk, S. V. Raghurame Rao

***A new discrete velocity method for Navier-Stokes equations***

The relation between the Lattice Boltzmann Method, which has recently become popular, and the Kinetic Schemes, which are routinely used in Computational Fluid Dynamics, is explored. A new discrete velocity model for the numerical solution of Navier-Stokes equations for incompressible fluid flow is presented by combining both the approaches. The new scheme can be interpreted as a pseudo-compressibility method and, for a particular choice of parameters, this interpretation carries over to the Lattice Boltzmann Method.
(20 pages, 1999)

16. H. Neunzert

***Mathematics as a Key to Key Technologies***

The main part of this paper will consist of examples, how mathematics really helps to solve industrial problems; these examples are taken from our Institute for Industrial Mathematics, from research in the Technomathematics group at my university, but also from ECMI groups and a company called TecMath, which originated 10 years ago from my university group and has already a very successful history.
(39 pages (4 PDF-Files), 1999)

17. J. Ohser, K. Sandau

***Considerations about the Estimation of the Size Distribution in Wicksell's Corpuscle Problem***

Wicksell's corpuscle problem deals with the estimation of the size distribution of a population of particles, all having the same shape, using a lower dimensional sampling probe. This problem was originary formulated for particle systems occurring in life sciences but its solution is of actual and increasing interest in materials science. From a mathematical point of view, Wicksell's problem is an inverse problem where the interesting size distribution is the unknown part of a Volterra equation. The problem is often regarded ill-posed, because the structure of the integrand implies unstable numerical solutions. The accuracy of the numerical solutions is considered here using the condition number, which allows to compare different numerical methods with different (equidistant) class sizes and which indicates, as one result, that a finite section thickness of the probe reduces the numerical problems. Furthermore, the relative error of estimation is computed which can be split into two parts. One part consists of the relative discretization error that increases for increasing class size, and the second part is related to the relative statistical error which increases with decreasing class size. For both parts, upper bounds can be given and the sum of them indicates an optimal class width depending on some specific constants.
(18 pages, 1999)

18. E. Carrizosa, H. W. Hamacher, R. Klein, S. Nickel

***Solving nonconvex planar location problems by finite dominating sets***

It is well-known that some of the classical location problems with polyhedral gauges can be solved in polynomial time by finding a finite dominating set, i.e. a finite set of candidates guaranteed to contain at least one optimal location.
In this paper it is first established that this result holds

for a much larger class of problems than currently considered in the literature. The model for which this result can be proven includes, for instance, location problems with attraction and repulsion, and location-allocation problems.
Next, it is shown that the approximation of general gauges by polyhedral ones in the objective function of our general model can be analyzed with regard to the subsequent error in the optimal objective value. For the approximation problem two different approaches are described, the sandwich procedure and the greedy algorithm. Both of these approaches lead - for fixed epsilon - to polynomial approximation algorithms with accuracy epsilon for solving the general model considered in this paper.
*Keywords: Continuous Location, Polyhedral Gauges, Finite Dominating Sets, Approximation, Sandwich Algorithm, Greedy Algorithm*
(19 pages, 2000)

19. A. Becker

***A Review on Image Distortion Measures***

Within this paper we review image distortion measures. A distortion measure is a criterion that assigns a "quality number" to an image. We distinguish between mathematical distortion measures and those distortion measures in-cooperating a priori knowledge about the imaging devices ( e. g. satellite images), image processing algorithms or the human physiology. We will consider representative examples of different kinds of distortion measures and are going to discuss them.
*Keywords: Distortion measure, human visual system*
(26 pages, 2000)

20. H. W. Hamacher, M. Labbé, S. Nickel, T. Sonneborn

**Polyhedral Properties of the Uncapacitated Multiple Allocation Hub Location Problem**

We examine the feasibility polyhedron of the uncapacitated hub location problem (UHL) with multiple allocation, which has applications in the fields of air passenger and cargo transportation, telecommunication and postal delivery services. In particular we determine the dimension and derive some classes of facets of this polyhedron. We develop some general rules about lifting facets from the uncapacitated facility location (UFL) for UHL and projecting facets from UHL to UFL. By applying these rules we get a new class of facets for UHL which dominates the inequalities in the original formulation. Thus we get a new formulation of UHL whose constraints are all facet–defining. We show its superior computational performance by benchmarking it on a well known data set.
*Keywords: integer programming, hub location, facility location, valid inequalities, facets, branch and cut*
(21 pages, 2000)

21. H. W. Hamacher, A. Schöbel

***Design of Zone Tariff Systems in Public Transportation***

Given a public transportation system represented by its stops and direct connections between stops, we consider two problems dealing with the prices for the customers: The fare problem in which subsets of stops are already aggregated to zones and "good" tariffs have to be found in the existing zone system. Closed form solutions for the fare problem are presented for three objective functions. In the zone problem the design of the zones is part of the problem. This problem is NP hard and we therefore propose three heuristics which prove to be very successful in the redesign of one of Germany's transportation systems.
(30 pages, 2001)

22. D. Hietel, M. Junk, R. Keck, D. Teleaga:

***The Finite-Volume-Particle Method for Conservation Laws***

In the Finite-Volume-Particle Method (FVPM), the weak formulation of a hyperbolic conservation law is discretized by restricting it to a discrete set of test functions. In contrast to the usual Finite-Volume approach, the test functions are not taken as characteristic functions of the control volumes in a spatial grid, but are chosen from a partition of unity with smooth and overlapping partition functions (the particles), which can even move along pre- scribed velocity fields. The information exchange between particles is based on standard numerical flux functions. Geometrical information, similar to the surface area of the cell faces in the Finite-Volume Method and the corresponding normal directions are given as integral quantities of the partition functions. After a brief derivation of the Finite-Volume-Particle Method, this work focuses on the role of the geometric coefficients in the scheme.
(16 pages, 2001)

23. T. Bender, H. Hennes, J. Kalcsics, M. T. Melo, S. Nickel

***Location Software and Interface with GIS and Supply Chain Management***

The objective of this paper is to bridge the gap between location theory and practice. To meet this objective focus is given to the development of software capable of addressing the different needs of a wide group of users. There is a very active community on location theory encompassing many research fields such as operations research, computer science, mathematics, engineering, geography, economics and marketing. As a result, people working on facility location problems have a very diverse background and also different needs regarding the software to solve these problems. For those interested in non-commercial applications (e. g. students and researchers), the library of location algorithms (LoLA can be of considerable assistance. LoLA contains a collection of efficient algorithms for solving planar, network and discrete facility location problems. In this paper, a detailed description of the functionality of LoLA is presented. In the fields of geography and marketing, for instance, solving facility location problems requires using large amounts of demographic data. Hence, members of these groups (e. g. urban planners and sales managers) often work with geographical information too s. To address the specific needs of these users, LoLA was inked to a geographical information system (GIS) and the details of the combined functionality are described in the paper. Finally, there is a wide group of practitioners who need to solve large problems and require special purpose software with a good data interface. Many of such users can be found, for example, in the area of supply chain management (SCM). Logistics activities involved in strategic SCM include, among others, facility location planning. In this paper, the development of a commercial location software tool is also described. The too is embedded in the Advanced Planner and Optimizer SCM software developed by SAP AG, Walldorf, Germany. The paper ends with some conclusions and an outlook to future activities.
*Keywords: facility location, software development, geographical information systems, supply chain management.*
(48 pages, 2001)

24. H. W. Hamacher, S. A. Tjandra

***Mathematical Modelling of Evacuation Problems: A State of Art***

This paper details models and algorithms which can be applied to evacuation problems. While it concentrates on building evacuation many of the results are applicable also to regional evacuation. All models consider the time as main parameter, where the travel time between components of the building is part of the input and the overall evacuation time is the output. The paper distinguishes between macroscopic and microscopic evacuation models both of which are able to capture the evacuees' movement over time.
Macroscopic models are mainly used to produce good lower bounds for the evacuation time and do not consider any individual behavior during the emergency situation. These bounds can be used to analyze existing buildings or help in the design phase of planning a building. Macroscopic approaches which are based on dynamic network flow models (minimum cost dynamic flow, maximum dynamic flow, universal maximum flow, quickest path and quickest flow) are described. A special feature of the presented approach is the fact, that travel times of evacuees are not restricted to be constant, but may be density dependent. Using multicriteria optimization priority regions and blockage due to fire or smoke may be considered. It is shown how the modelling can be done using time parameter either as discrete or continuous parameter.
Microscopic models are able to model the individual evacuee's characteristics and the interaction among evacuees which influence their movement. Due to the corresponding huge amount of data one uses simulation approaches. Some probabilistic laws for individual evacuee's movement are presented. Moreover ideas to model the evacuee's movement using cellular automata (CA) and resulting software are presented. In this paper we will focus on macroscopic models and only summarize some of the results of the microscopic approach. While most of the results are applicable to general evacuation situations, we concentrate on building evacuation.
(44 pages, 2001)

25. J. Kuhnert, S. Tiwari

***Grid free method for solving the Poisson equation***

A Grid free method for solving the Poisson equation is presented. This is an iterative method. The method is based on the weighted least squares approximation in which the Poisson equation is enforced to be satisfied in every iterations. The boundary conditions can also be enforced in the iteration process. This is a local approximation procedure. The Dirichlet, Neumann and mixed boundary value problems on a unit square are presented and the analytical solutions are compared with the exact solutions. Both solutions matched perfectly.
*Keywords: Poisson equation, Least squares method, Grid free method*
(19 pages, 2001)

26. T. Götz, H. Rave, D. Reinel-Bitzer, K. Steiner, H. Tiemeier

***Simulation of the fiber spinning process***

To simulate the influence of process parameters to the melt spinning process a fiber model is used and coupled with CFD calculations of the quench air flow. In the fiber model energy, momentum and mass balance are solved for the polymer mass flow. To calculate the quench air the Lattice Boltzmann method is used. Simulations and experiments for different process parameters and hole configurations are compared and show a good agreement.

*Keywords: Melt spinning, fiber model, Lattice Boltzmann, CFD*

(19 pages, 2001)

27. A. Zemitis

***On interaction of a liquid film with an obstacle***

In this paper mathematical models for liquid films generated by impinging jets are discussed. Attention is stressed to the interaction of the liquid film with some obstacle. S. G. Taylor [Proc. R. Soc. London Ser. A 253, 313 (1959)] found that the liquid film generated by impinging jets is very sensitive to properties of the wire which was used as an obstacle. The aim of this presentation is to propose a modification of the Taylor's model, which allows to simulate the film shape in cases, when the angle between jets is different from 180°. Numerical results obtained by discussed models give two different shapes of the liquid film similar as in Taylors experiments. These two shapes depend on the regime: either droplets are produced close to the obstacle or not. The difference between two regimes becomes larger if the angle between jets decreases. Existence of such two regimes can be very essential for some applications of impinging jets, if the generated liquid film can have a contact with obstacles.

*Keywords: impinging jets, liquid film, models, numerical solution, shape*

(22 pages, 2001)

28. I. Ginzburg, K. Steiner

***Free surface lattice-Boltzmann method to model the filling of expanding cavities by Bingham Fluids***

The filling process of viscoplastic metal alloys and plastics in expanding cavities is modelled using the lattice Boltzmann method in two and three dimensions. These models combine the regularized Bingham model for viscoplastic with a free-interface algorithm. The latter is based on a modified immiscible lattice Boltzmann model in which one species is the fluid and the other one is considered as vacuum. The boundary conditions at the curved liquid-vacuum interface are met without any geometrical front reconstruction from a first-order Chapman-Enskog expansion. The numerical results obtained with these models are found in good agreement with available theoretical and numerical analysis.

*Keywords: Generalized LBE, free-surface phenomena, interface boundary conditions, filling processes, Bingham viscoplastic model, regularized models*

(22 pages, 2001)

29. H. Neunzert

***»Denn nichts ist für den Menschen als Menschen etwas wert, was er nicht mit Leidenschaft tun kann«***

Vortrag anlässlich der Verleihung des Akademiepreises des Landes Rheinland-Pfalz am 21.11.2001

Was macht einen guten Hochschullehrer aus? Auf diese Frage gibt es sicher viele verschiedene, fachbezogene Antworten, aber auch ein paar allgemeine Gesichtspunkte: es bedarf der »Leidenschaft« für die Forschung (Max Weber), aus der dann auch die Begeisterung für die Lehre erwächst. Forschung und Lehre gehören zusammen, um die Wissenschaft als lebendiges Tun vermitteln zu können. Der Vortrag gibt Beispiele dafür, wie in angewandter Mathematik Forschungsaufgaben aus praktischen Alltagsproblemstellungen erwachsen, die in die Lehre auf verschiedenen Stufen (Gymnasium bis Graduiertenkolleg) einfließen; er leitet damit auch zu einem aktuellen Forschungsgebiet, der Mehrskalenanalyse mit ihren vielfältigen Anwendungen in Bildverarbeitung, Materialentwicklung und Strömungsmechanik über, was aber nur kurz gestreift wird. Mathematik erscheint hier als eine moderne Schlüsseltechnologie, die aber auch enge Beziehungen zu den Geistes- und Sozialwissenschaften hat.

*Keywords: Lehre, Forschung, angewandte Mathematik, Mehrskalenanalyse, Strömungsmechanik*

(18 pages, 2001)

30. J. Kuhnert, S. Tiwari

***Finite pointset method based on the projection method for simulations of the incompressible Navier-Stokes equations***

A Lagrangian particle scheme is applied to the projection method for the incompressible Navier-Stokes equations. The approximation of spatial derivatives is obtained by the weighted least squares method. The pressure Poisson equation is solved by a local iterative procedure with the help of the least squares method. Numerical tests are performed for two dimensional cases. The Couette flow, Poiseuelle flow, decaying shear flow and the driven cavity flow are presented. The numerical solutions are obtained for stationary as well as instationary cases and are compared with the analytical solutions for channel flows. Finally, the driven cavity in a unit square is considered and the stationary solution obtained from this scheme is compared with that from the finite element method.

*Keywords: Incompressible Navier-Stokes equations, Meshfree method, Projection method, Particle scheme, Least squares approximation*

*AMS subject classification: 76D05, 76M28*

(25 pages, 2001)

31. R. Korn, M. Krekel

***Optimal Portfolios with Fixed Consumption or Income Streams***

We consider some portfolio optimisation problems where either the investor has a desire for an a priori specified consumption stream or/and follows a deterministic pay in scheme while also trying to maximize expected utility from final wealth. We derive explicit closed form solutions for continuous and discrete monetary streams. The mathematical method used is classical stochastic control theory.

*Keywords: Portfolio optimisation, stochastic control, HJB equation, discretisation of control problems.*

(23 pages, 2002)

32. M. Krekel

***Optimal portfolios with a loan dependent credit spread***

If an investor borrows money he generally has to pay higher interest rates than he would have received, if he had put his funds on a savings account. The classical model of continuous time portfolio optimisation ignores this effect. Since there is obviously a connection between the default probability and the total percentage of wealth, which the investor is in debt, we study portfolio optimisation with a control dependent interest rate. Assuming a logarithmic and a power utility function, respectively, we prove explicit formulae of the optimal control.

*Keywords: Portfolio optimisation, stochastic control, HJB equation, credit spread, log utility, power utility, non-linear wealth dynamics*

(25 pages, 2002)

33. J. Ohser, W. Nagel, K. Schladitz

***The Euler number of discretized sets - on the choice of adjacency in homogeneous lattices***

Two approaches for determining the Euler-Poincaré characteristic of a set observed on lattice points are considered in the context of image analysis { the integral geometric and the polyhedral approach. Information about the set is assumed to be available on lattice points only. In order to retain properties of the Euler number and to provide a good approximation of the true Euler number of the original set in the Euclidean space, the appropriate choice of adjacency in the lattice for the set and its background is crucial. Adjacencies are defined using tessellations of the whole space into polyhedrons. In R 3 , two new 14 adjacencies are introduced additionally to the well known 6 and 26 adjacencies. For the Euler number of a set and its complement, a consistency relation holds. Each of the pairs of adjacencies (14:1; 14:1), (14:2; 14:2), (6; 26), and (26; 6) is shown to be a pair of complementary adjacencies with respect to this relation. That is, the approximations of the Euler numbers are consistent if the set and its background (complement) are equipped with this pair of adjacencies. Furthermore, sufficient conditions for the correctness of the approximations of the Euler number are given. The analysis of selected microstructures and a simulation study illustrate how the estimated Euler number depends on the chosen adjacency. It also shows that there is not a uniquely best pair of adjacencies with respect to the estimation of the Euler number of a set in Euclidean space.

*Keywords: image analysis, Euler number, neighborhod relationships, cuboidal lattice*

(32 pages, 2002)

34. I. Ginzburg, K. Steiner

***Lattice Boltzmann Model for Free-Surface flow and Its Application to Filling Process in Casting***

A generalized lattice Boltzmann model to simulate free-surface is constructed in both two and three dimensions. The proposed model satisfies the interfacial boundary conditions accurately. A distinctive feature of the model is that the collision processes is carried out only on the points occupied partially or fully by the fluid. To maintain a sharp interfacial front, the method includes an anti-diffusion algorithm. The unknown distribution functions at the interfacial region are constructed according to the first order Chapman-Enskog analysis. The interfacial boundary conditions are satis-

fied exactly by the coefficients in the Chapman-Enskog expansion. The distribution functions are naturally expressed in the local interfacial coordinates. The macroscopic quantities at the interface are extracted from the least-square solutions of a locally linearized system obtained from the known distribution functions. The proposed method does not require any geometric front construction and is robust for any interfacial topology. Simulation results of realistic filling process are presented: rectangular cavity in two dimensions and Hammer box, Campbell box, Sheffield box, and Motorblock in three dimensions. To enhance the stability at high Reynolds numbers, various upwind-type schemes are developed. Free-slip and no-slip boundary conditions are also discussed.
*Keywords: Lattice Boltzmann models; free-surface phenomena; interface boundary conditions; filling processes; injection molding; volume of fluid method; interface boundary conditions; advection-schemes; upwind-schemes*
(54 pages, 2002)

35. M. Günther, A. Klar, T. Materne, R. Wegener

***Multivalued fundamental diagrams and stop and go waves for continuum traffic equations***

In the present paper a kinetic model for vehicular traffic leading to multivalued fundamental diagrams is developed and investigated in detail. For this model phase transitions can appear depending on the local density and velocity of the flow. A derivation of associated macroscopic traffic equations from the kinetic equation is given. Moreover, numerical experiments show the appearance of stop and go waves for highway traffic with a bottleneck.
*Keywords: traffic flow, macroscopic equations, kinetic derivation, multivalued fundamental diagram, stop and go waves, phase transitions*
(25 pages, 2002)

36. S. Feldmann, P. Lang, D. Prätzel-Wolters

***Parameter influence on the zeros of network determinants***

To a network N($q$) with determinant D($s$;$q$) depending on a parameter vector $q \hat{I} R^r$ via identification of some of its vertices, a network N^ ($q$) is assigned. The paper deals with procedures to find N^ ($q$), such that its determinant D^ ($s$;$q$) admits a factorization in the determinants of appropriate subnetworks, and with the estimation of the deviation of the zeros of D^ from the zeros of D. To solve the estimation problem state space methods are applied.
*Keywords: Networks, Equicofactor matrix polynomials, Realization theory, Matrix perturbation theory*
(30 pages, 2002)

37. K. Koch, J. Ohser, K. Schladitz

***Spectral theory for random closed sets and estimating the covariance via frequency space***

A spectral theory for stationary random closed sets is developed and provided with a sound mathematical basis. Definition and proof of existence of the Bartlett spectrum of a stationary random closed set as well as the proof of a Wiener-Khintchine theorem for the power spectrum are used to two ends: First, well known second order characteristics like the covariance can be estimated faster than usual via frequency space. Second, the Bartlett spectrum and the power spectrum can be used as second order characteristics in frequency space. Examples show, that in some cases information about the random closed set is easier to obtain from these characteristics in frequency space than from their real world counterparts.
*Keywords: Random set, Bartlett spectrum, fast Fourier transform, power spectrum*
(28 pages, 2002)

38. D. d'Humières, I. Ginzburg

***Multi-reflection boundary conditions for lattice Boltzmann models***

We present a unified approach of several boundary conditions for lattice Boltzmann models. Its general framework is a generalization of previously introduced schemes such as the bounce-back rule, linear or quadratic interpolations, etc. The objectives are two fold: first to give theoretical tools to study the existing boundary conditions and their corresponding accuracy; secondly to design formally third- order accurate boundary conditions for general flows. Using these boundary conditions, Couette and Poiseuille flows are exact solution of the lattice Boltzmann models for a Reynolds number $Re = 0$ (Stokes limit).
Numerical comparisons are given for Stokes flows in periodic arrays of spheres and cylinders, linear periodic array of cylinders between moving plates and for Navier-Stokes flows in periodic arrays of cylinders for $Re < 200$. These results show a significant improvement of the overall accuracy when using the linear interpolations instead of the bounce-back reflection (up to an order of magnitude on the hydrodynamics fields). Further improvement is achieved with the new multi-reflection boundary conditions, reaching a level of accuracy close to the quasi-analytical reference solutions, even for rather modest grid resolutions and few points in the narrowest channels. More important, the pressure and velocity fields in the vicinity of the obstacles are much smoother with multi-reflection than with the other boundary conditions.
Finally the good stability of these schemes is highlighted by some simulations of moving obstacles: a cylinder between flat walls and a sphere in a cylinder.
*Keywords: lattice Boltzmann equation, boudary condistions, bounce-back rule, Navier-Stokes equation*
(72 pages, 2002)

39. R. Korn

***Elementare Finanzmathematik***

Im Rahmen dieser Arbeit soll eine elementar gehaltene Einführung in die Aufgabenstellungen und Prinzipien der modernen Finanzmathematik gegeben werden. Insbesondere werden die Grundlagen der Modellierung von Aktienkursen, der Bewertung von Optionen und der Portfolio-Optimierung vorgestellt. Natürlich können die verwendeten Methoden und die entwickelte Theorie nicht in voller Allgemeinheit für den Schulunterricht verwendet werden, doch sollen einzelne Prinzipien so heraus gearbeitet werden, dass sie auch an einfachen Beispielen verstanden werden können.
*Keywords: Finanzmathematik, Aktien, Optionen, Portfolio-Optimierung, Börse, Lehrerweiterbildung, Mathematikunterricht*
(98 pages, 2002)

40. J. Kallrath, M. C. Müller, S. Nickel

***Batch Presorting Problems: Models and Complexity Results***

In this paper we consider short term storage systems. We analyze presorting strategies to improve the effiency of these storage systems. The presorting task is called Batch PreSorting Problem (BPSP). The BPSP is a variation of an assigment problem, i. e., it has an assigment problem kernel and some additional constraints. We present different types of these presorting problems, introduce mathematical programming formulations and prove the NP-completeness for one type of the BPSP. Experiments are carried out in order to compare the different model formulations and to investigate the behavior of these models.
*Keywords: Complexity theory, Integer programming, Assigment, Logistics*
(19 pages, 2002)

41. J. Linn

***On the frame-invariant description of the phase space of the Folgar-Tucker equation***

The Folgar-Tucker equation is used in flow simulations of fiber suspensions to predict fiber orientation depending on the local flow. In this paper, a complete, frame-invariant description of the phase space of this differential equation is presented for the first time.
*Key words: fiber orientation, Folgar-Tucker equation, injection molding*
(5 pages, 2003)

42. T. Hanne, S. Nickel

***A Multi-Objective Evolutionary Algorithm for Scheduling and Inspection Planning in Software Development Projects***

In this article, we consider the problem of planning inspections and other tasks within a software development (SD) project with respect to the objectives quality (no. of defects), project duration, and costs. Based on a discrete-event simulation model of SD processes comprising the phases coding, inspection, test, and rework, we present a simplified formulation of the problem as a multiobjective optimization problem. For solving the problem (i. e. finding an approximation of the efficient set) we develop a multiobjective evolutionary algorithm. Details of the algorithm are discussed as well as results of its application to sample problems.
*Key words: multiple objective programming, project management and scheduling, software development, evolutionary algorithms, efficient set*
(29 pages, 2003)

43. T. Bortfeld , K.-H. Küfer, M. Monz, A. Scherrer, C. Thieke, H. Trinkaus

***Intensity-Modulated Radiotherapy - A Large Scale Multi-Criteria Programming Problem -***

Radiation therapy planning is always a tight rope walk between dangerous insufficient dose in the target volume and life threatening overdosing of organs at risk. Finding ideal balances between these inherently contradictory goals challenges dosimetrists and physicians in their daily practice. Today's planning systems are typically based on a single evaluation function that measures the quality of a radiation treatment plan. Unfortunately, such a one dimensional approach can-

not satisfactorily map the different backgrounds of physicians and the patient dependent necessities. So, too often a time consuming iteration process between evaluation of dose distribution and redefinition of the evaluation function is needed.
In this paper we propose a generic multi-criteria approach based on Pareto's solution concept. For each entity of interest - target volume or organ at risk a structure dependent evaluation function is defined measuring deviations from ideal doses that are calculated from statistical functions. A reasonable bunch of clinically meaningful Pareto optimal solutions are stored in a data base, which can be interactively searched by physicians. The system guarantees dynamical planning as well as the discussion of tradeoffs between different entities.
Mathematically, we model the upcoming inverse problem as a multi-criteria linear programming problem. Because of the large scale nature of the problem it is not possible to solve the problem in a 3D-setting without adaptive reduction by appropriate approximation schemes.
Our approach is twofold: First, the discretization of the continuous problem is based on an adaptive hierarchical clustering process which is used for a local refinement of constraints during the optimization procedure. Second, the set of Pareto optimal solutions is approximated by an adaptive grid of representatives that are found by a hybrid process of calculating extreme compromises and interpolation methods.
*Keywords: multiple criteria optimization, representative systems of Pareto solutions, adaptive triangulation, clustering and disaggregation techniques, visualization of Pareto solutions, medical physics, external beam radiotherapy planning, intensity modulated radiotherapy*
(31 pages, 2003)

44. T. Halfmann, T. Wichmann

***Overview of Symbolic Methods in Industrial Analog Circuit Design***

Industrial analog circuits are usually designed using numerical simulation tools. To obtain a deeper circuit understanding, symbolic analysis techniques can additionally be applied. Approximation methods which reduce the complexity of symbolic expressions are needed in order to handle industrial-sized problems. This paper will give an overview to the field of symbolic analog circuit analysis. Starting with a motivation, the state-of-the-art simplification algorithms for linear as well as for nonlinear circuits are presented. The basic ideas behind the different techniques are described, whereas the technical details can be found in the cited references. Finally, the application of linear and nonlinear symbolic analysis will be shown on two example circuits.
*Keywords: CAD, automated analog circuit design, symbolic analysis, computer algebra, behavioral modeling, system simulation, circuit sizing, macro modeling, differential-algebraic equations, index*
(17 pages, 2003)

45. S. E. Mikhailov, J. Orlik

***Asymptotic Homogenisation in Strength and Fatigue Durability Analysis of Composites***

Asymptotic homogenisation technique and two-scale convergence is used for analysis of macro-strength and fatigue durability of composites with a periodic structure under cyclic loading. The linear damage accumulation rule is employed in the phenomenological micro-durability conditions (for each component of the composite) under varying cyclic loading. Both local and non-local strength and durability conditions are analysed. The strong convergence of the strength and fatigue damage measure as the structure period tends to zero is proved and their limiting values are estimated.
*Keywords: multiscale structures, asymptotic homogenization, strength, fatigue, singularity, non-local conditions*
(14 pages, 2003)

46. P. Domínguez-Marín, P. Hansen, N. Mladenović, S. Nickel

***Heuristic Procedures for Solving the Discrete Ordered Median Problem***

We present two heuristic methods for solving the Discrete Ordered Median Problem (DOMP), for which no such approaches have been developed so far. The DOMP generalizes classical discrete facility location problems, such as the p-median, p-center and Uncapacitated Facility Location problems. The first procedure proposed in this paper is based on a genetic algorithm developed by Moreno Vega [MV96] for p-median and p-center problems. Additionally, a second heuristic approach based on the Variable Neighborhood Search metaheuristic (VNS) proposed by Hansen & Mladenovic [HM97] for the p-median problem is described. An extensive numerical study is presented to show the efficiency of both heuristics and compare them.
*Keywords: genetic algorithms, variable neighborhood search, discrete facility location*
(31 pages, 2003)

47. N. Boland, P. Domínguez-Marín, S. Nickel, J. Puerto

***Exact Procedures for Solving the Discrete Ordered Median Problem***

The Discrete Ordered Median Problem (DOMP) generalizes classical discrete location problems, such as the N-median, N-center and Uncapacitated Facility Location problems. It was introduced by Nickel [16], who formulated it as both a nonlinear and a linear integer program. We propose an alternative integer linear programming formulation for the DOMP, discuss relationships between both integer linear programming formulations, and show how properties of optimal solutions can be used to strengthen these formulations. Moreover, we present a specific branch and bound procedure to solve the DOMP more efficiently. We test the integer linear programming formulations and this branch and bound method computationally on randomly generated test problems.
*Keywords: discrete location, Integer programming*
(41 pages, 2003)

48. S. Feldmann, P. Lang

***Padé-like reduction of stable discrete linear systems preserving their stability***

A new stability preserving model reduction algorithm for discrete linear SISO-systems based on their impulse response is proposed. Similar to the Padé approximation, an equation system for the Markov parameters involving the Hankel matrix is considered, that here however is chosen to be of very high dimension. Although this equation system therefore in general cannot be solved exactly, it is proved that the approximate solution, computed via the Moore-Penrose inverse, gives rise to a stability preserving reduction scheme, a property that cannot be guaranteed for the Padé approach. Furthermore, the proposed algorithm is compared to another stability preserving reduction approach, namely the balanced truncation method, showing comparable performance of the reduced systems. The balanced truncation method however starts from a state space description of the systems and in general is expected to be more computational demanding.
*Keywords: Discrete linear systems, model reduction, stability, Hankel matrix, Stein equation*
(16 pages, 2003)

49. J. Kallrath, S. Nickel

***A Polynomial Case of the Batch Presorting Problem***

This paper presents new theoretical results for a special case of the batch presorting problem (BPSP). We will show tht this case can be solved in polynomial time. Offline and online algorithms are presented for solving the BPSP. Competetive analysis is used for comparing the algorithms.
*Keywords: batch presorting problem, online optimization, competetive analysis, polynomial algorithms, logistics*
(17 pages, 2003)

50. T. Hanne, H. L. Trinkaus

***knowCube for MCDM – Visual and Interactive Support for Multicriteria Decision Making***

In this paper, we present a novel multicriteria decision support system (MCDSS), called knowCube, consisting of components for knowledge organization, generation, and navigation. Knowledge organization rests upon a database for managing qualitative and quantitative criteria, together with add-on information. Knowledge generation serves filling the database via e. g. identification, optimization, classification or simulation. For "finding needles in haycocks", the knowledge navigation component supports graphical database retrieval and interactive, goal-oriented problem solving. Navigation "helpers" are, for instance, cascading criteria aggregations, modifiable metrics, ergonomic interfaces, and customizable visualizations. Examples from real-life projects, e.g. in industrial engineering and in the life sciences, illustrate the application of our MCDSS.
*Key words: Multicriteria decision making, knowledge management, decision support systems, visual interfaces, interactive navigation, real-life applications.*
(26 pages, 2003)

51. O. Iliev, V. Laptev

***On Numerical Simulation of Flow Through Oil Filters***

This paper concerns numerical simulation of flow through oil filters. Oil filters consist of filter housing (filter box), and a porous filtering medium, which completely separates the inlet from the outlet. We discuss mathematical models, describing coupled flows in the pure liquid subregions and in the porous filter media, as well as interface conditions between them. Further, we reformulate the problem in fictitious regions method manner, and discuss peculiarities of the numerical algorithm in solving the coupled system. Next, we show numerical results, validating the model and the

algorithm. Finally, we present results from simulation of 3-D oil flow through a real car filter.
*Keywords: oil filters, coupled flow in plain and porous media, Navier-Stokes, Brinkman, numerical simulation*
(8 pages, 2003)

52. W. Dörfler, O. Iliev, D. Stoyanov, D. Vassileva

***On a Multigrid Adaptive Refinement Solver for Saturated Non-Newtonian Flow in Porous Media***

A multigrid adaptive refinement algorithm for non-Newtonian flow in porous media is presented. The saturated flow of a non-Newtonian fluid is described by the continuity equation and the generalized Darcy law. The resulting second order nonlinear elliptic equation is discretized by a finite volume method on a cell-centered grid. A nonlinear full-multigrid, full-approximation-storage algorithm is implemented. As a smoother, a single grid solver based on Picard linearization and Gauss-Seidel relaxation is used. Further, a local refinement multigrid algorithm on a composite grid is developed. A residual based error indicator is used in the adaptive refinement criterion. A special implementation approach is used, which allows us to perform unstructured local refinement in conjunction with the finite volume discretization. Several results from numerical experiments are presented in order to examine the performance of the solver.
*Keywords: Nonlinear multigrid, adaptive refinement, non-Newtonian flow in porous media*
(17 pages, 2003)

53. S. Kruse

***On the Pricing of Forward Starting Options under Stochastic Volatility***

We consider the problem of pricing European forward starting options in the presence of stochastic volatility. By performing a change of measure using the asset price at the time of strike determination as a numeraire, we derive a closed-form solution based on Heston's model of stochastic volatility.
*Keywords: Option pricing, forward starting options, Heston model, stochastic volatility, cliquet options*
(11 pages, 2003)

54. O. Iliev, D. Stoyanov

***Multigrid – adaptive local refinement solver for incompressible flows***

A non-linear multigrid solver for incompressible Navier-Stokes equations, exploiting finite volume discretization of the equations, is extended by adaptive local refinement. The multigrid is the outer iterative cycle, while the SIMPLE algorithm is used as a smoothing procedure. Error indicators are used to define the refinement subdomain. A special implementation approach is used, which allows to perform unstructured local refinement in conjunction with the finite volume discretization. The multigrid - adaptive local refinement algorithm is tested on 2D Poisson equation and further is applied to a lid-driven flows in a cavity (2D and 3D case), comparing the results with bench-mark data. The software design principles of the solver are also discussed.
*Keywords: Navier-Stokes equations, incompressible flow, projection-type splitting, SIMPLE, multigrid methods, adaptive local refinement, lid-driven flow in a cavity*
(37 pages, 2003)

55. V. Starikovicius

***The multiphase flow and heat transfer in porous media***

In first part of this work, summaries of traditional Multiphase Flow Model and more recent Multiphase Mixture Model are presented. Attention is being paid to attempts include various heterogeneous aspects into models. In second part, MMM based differential model for two-phase immiscible flow in porous media is considered. A numerical scheme based on the sequential solution procedure and control volume based finite difference schemes for the pressure and saturation-conservation equations is developed. A computer simulator is built, which exploits object-oriented programming techniques. Numerical result for several test problems are reported.
*Keywords: Two-phase flow in porous media, various formulations, global pressure, multiphase mixture model, numerical simulation*
(30 pages, 2003)

56. P. Lang, A. Sarishvili, A. Wirsen

***Blocked neural networks for knowledge extraction in the software development process***

One of the main goals of an organization developing software is to increase the quality of the software while at the same time to decrease the costs and the duration of the development process. To achieve this, various decisions e.ecting this goal before and during the development process have to be made by the managers. One appropriate tool for decision support are simulation models of the software life cycle, which also help to understand the dynamics of the software development process. Building up a simulation model requires a mathematical description of the interactions between di.erent objects involved in the development process. Based on experimental data, techniques from the .eld of knowledge discovery can be used to quantify these interactions and to generate new process knowledge based on the analysis of the determined relationships. In this paper blocked neuronal networks and related relevance measures will be presented as an appropriate tool for quanti.cation and validation of qualitatively known dependencies in the software development process.
*Keywords: Blocked Neural Networks, Nonlinear Regression, Knowledge Extraction, Code Inspection*
(21 pages, 2003)

57. H. Knaf, P. Lang, S. Zeiser

***Diagnosis aiding in Regulation Thermography using Fuzzy Logic***

The objective of the present article is to give an overview of an application of Fuzzy Logic in Regulation Thermography, a method of medical diagnosis support. An introduction to this method of the complementary medical science based on temperature measurements – so-called thermograms – is provided. The process of modelling the physician's thermogram evaluation rules using the calculus of Fuzzy Logic is explained.
*Keywords: fuzzy logic,knowledge representation, expert system*
(22 pages, 2003)

58. M.T. Melo, S. Nickel, F. Saldanha da Gama

***Largescale models for dynamic multi-commodity capacitated facility location***

In this paper we focus on the strategic design of supply chain networks. We propose a mathematical modeling framework that captures many practical aspects of network design problems simultaneously but which have not received adequate attention in the literature. The aspects considered include: dynamic planning horizon, generic supply chain network structure, external supply of materials, inventory opportunities for goods, distribution of commodities, facility configuration, availability of capital for investments, and storage limitations. Moreover, network configuration decisions concerning the gradual relocation of facilities over the planning horizon are considered. To cope with fluctuating demands, capacity expansion and reduction scenarios are also analyzed as well as modular capacity shifts. The relation of the proposed modeling framework with existing models is discussed. For problems of reasonable size we report on our computational experience with standard mathematical programming software. In particular, useful insights on the impact of various factors on network design decisions are provided.
*Keywords: supply chain management, strategic planning, dynamic location, modeling*
(40 pages, 2003)

59. J. Orlik

***Homogenization for contact problems with periodically rough surfaces***

We consider the contact of two elastic bodies with rough surfaces at the interface. The size of the micro-peaks and valleys is very small compared with the macrosize of the bodies' domains. This makes the direct application of the FEM for the calculation of the contact problem prohibitively costly. A method is developed that allows deriving a macrocontact condition on the interface. The method involves the twoscale asymptotic homogenization procedure that takes into account the microgeometry of the interface layer and the stiffnesses of materials of both domains. The macrocontact condition can then be used in a FEM model for the contact problem on the macrolevel. The averaged contact stiffness obtained allows the replacement of the interface layer in the macromodel by the macrocontact condition.
*Keywords: asymptotic homogenization, contact problems*
(28 pages, 2004)

60. A. Scherrer, K.-H. Küfer, M. Monz, F. Alonso, T. Bortfeld

***IMRT planning on adaptive volume structures – a significant advance of computational complexity***

In intensity-modulated radiotherapy (IMRT) planning the oncologist faces the challenging task of finding a treatment plan that he considers to be an ideal compromise of the inherently contradictive goals of delivering a sufficiently high dose to the target while widely sparing critical structures. The search for this a priori unknown compromise typically requires the computation of several plans, i.e. the solution of several optimization problems. This accumulates to a high computa-

tional expense due to the large scale of these problems - a consequence of the discrete problem formulation. This paper presents the adaptive clustering method as a new algorithmic concept to overcome these difficulties. The computations are performed on an individually adapted structure of voxel clusters rather than on the original voxels leading to a decisively reduced computational complexity as numerical examples on real clinical data demonstrate. In contrast to many other similar concepts, the typical trade-off between a reduction in computational complexity and a loss in exactness can be avoided: the adaptive clustering method produces the optimum of the original problem. This flexible method can be applied to both single- and multi-criteria optimization methods based on most of the convex evaluation functions used in practice.
*Keywords: Intensity-modulated radiation therapy (IMRT), inverse treatment planning, adaptive volume structures, hierarchical clustering, local refinement, adaptive clustering, convex programming, mesh generation, multi-grid methods*
(24 pages, 2004)

Status quo: April 2004